

Spatio-temporal characterization of a complete algal bloom event using fluorescence spectroscopy in tandem with conventional physico-chemical methods

by

Emily Randig

B.S., California State Polytechnic University, Pomona, 2020

A THESIS

submitted in partial fulfillment of the requirements for the degree

MASTER OF SCIENCE

Department of Civil Engineering
Carl R. Ice College of Engineering

KANSAS STATE UNIVERSITY
Manhattan, Kansas

2022

Approved by:

Major Professor
Prathap Parameswaran, PhD

Copyright

© Emily Randig 2022.

Abstract

An increase in the frequency and geographic distribution of algal and cyanobacterial blooms has been observed over the last two decades, threatening marine and freshwater ecosystems. In situ fluorometers have been proposed for their potential to provide early warning of bloom development through the analysis of fluorescence signatures of the water. Despite the potential of the technology, there has been no in-depth analysis studying the fluorescence and 3-D excitation emission matrixes (EEMs) in a waterbody experiencing an algal bloom with intensive monitoring. Furthermore, the correlations between the EEMs and other physical and chemical parameters of blooms have not been elucidated till date.

The Milford Gathering Pond in Geary County, KS experiences annual algal blooms that cause public access closures and affects the Kansas Department of Wildlife, Parks, and Tourism (KDWPT) fish hatchery. An algal bloom at the pond was intensively monitored from April 2021 to November 2021. Various water quality parameters such as pH, turbidity, orthophosphate, total filtered nitrogen, and total filtered carbon were tracked, and the 3-D fluorescence EEM spectroscopy was analyzed. Water quality parameters confirmed bloom development and proliferation through an observed logarithmic change in turbidity, increase in pH above 9, and decrease in orthophosphate. EEM intensity changes were traced through both visual peak identification and with Parallel Factor Analysis (PARAFAC). Two peaks were identified visually: Peak C and Peak T. PARAFAC identified three fluorescence components with compound peaks. Component 1 had Peak A and Peak C1, component 2 had Peak A and Peak C2, and Component 3 had Peak T1 and Peak T2. Peaks A and C represent humic-like compounds and Peak T represents tryptophan like compounds. The visually identified T peak and PARAFAC component C3 representing tryptophan-like fluorescence were shown to be the best

predictor of algal bloom severity and progression with high correlations to pH, turbidity, and orthophosphate. In addition, the tryptophan-like fluorescence showed an increase in intensity before the onset of the bloom event, signaled by the jump in turbidity. This suggests that tryptophan-like fluorescence can be used as a predictive indicator of bloom proliferation. The findings show promise for a proactive and realistic algal monitoring tool which can be used by regulators and scientists alike for greater societal and environmental well-being.

Table of Contents

List of Figures	vii
List of Tables	ix
Acknowledgements	x
Chapter 1 - Introduction.....	1
Background.....	1
Research Objectives.....	2
Chapter 2 - Literature Review.....	3
Freshwater Harmful Algal Blooms.....	3
What are Algal Blooms?.....	3
Factors Contributing to Blooms.....	4
Fertilizer Runoff.....	5
Animal Feeding Operations (AFOs).....	5
Wastewater Pollution	6
Atmospheric Deposition of Nutrients	6
Hydrologic Changes.....	7
Climate Change.....	7
Effects of Algal Blooms.....	8
Human Health Impacts	8
Aquatic Ecosystem Health Impacts	9
Economic Impacts.....	9
Bloom Prevention and Mitigation.....	10
Physical Control.....	10
Mechanical Control.....	11
Biological Control.....	11
Chemical Control	12
Environmental Control.....	12
Conventional Bloom Detection and Monitoring	13
Principles of Fluorescence Spectroscopy for Monitoring Organic Matter	14
Evaluation of EEMs through Parallel Factor Analysis	15

Inferences and Knowledge Gaps	20
Chapter 3 - The Milford Gathering Pond.....	21
Chapter 4 - Materials and Methods.....	25
Sample Collection.....	25
Meteorologic Data Collection.....	27
Measurements of Temperature, pH, Turbidity, Orthophosphate, Total	27
Carbon, and Total Nitrogen	27
Fluorescence EEM-PARAFAC Analysis	27
Chapter 5 - Results and Discussion	31
Meteorologic and Environmental Conditions.....	31
Water Quality Parameters.....	34
Turbidity	34
Water Temperature	36
pH.....	37
Orthophosphate	38
Filtered Total Carbon	40
Filtered Total Nitrogen	41
Fluorescence Spectroscopy EEMs and PARAFAC Analysis.....	43
PARAFAC Components and Analysis	43
Changes in EEM Spectra and Fluorescence Intensity for Visually Identified Peaks	47
T peak Intensity as a Predictive Indicator of Bloom Proliferation	48
Correlations Between Parameters of Interest.....	50
Chapter 6 - Conclusion	55
References.....	57
Appendix A - PARAFAC Identified Outliers.....	1

List of Figures

Figure 2.1: Algal Paint-like Slicks and Scums Observed in the Milford Gathering Pond	3
Figure 2.2: EEM Visualization (Hansen et al., 2018).....	15
Figure 3.1: Location Map of Milford Lake and the Milford Gathering Pond	21
Figure 3.2: Milford Dam Cross Section (Stark et al., 2011).....	22
Figure 3.3: Timeline of KDHE Established HAB Watch and Warning in the Milford Gathering Pond	23
Figure 3.4: KDHE HAB Response Program Sampling Data for the Milford Gathering Pond in 2021.....	24
Figure 4.1: Sampling Site Location Map.....	25
Figure 4.2: Panoramic Pictures of Sampling Sites.....	26
Figure 4.3: PARAFAC 3 Component Model Leverages and Loadings	29
Figure 4.4: OpenFluor PARAFAC Component Matches	30
Figure 5.1: Precipitation Data.....	31
Figure 5.2: Air Temperature Data.....	32
Figure 5.3: Algal Scum Accumulation Observed on June 3 rd at Site B.....	33
Figure 5.4: Mean Daily Wind Speed at 2m	33
Figure 5.5: Solar Radiation Data	34
Figure 5.6: Visual Example of Turbidity within the Gathering Pond on June 15 th	35
Figure 5.7: Turbidity and Cell Count Data	35
Figure 5.8: Water Temperature Data	36
Figure 5.9: pH Data.....	37
Figure 5.10: Orthophosphate as PO ₄ -P	39
Figure 5.11: Filtered Total Carbon	41
Figure 5.12: Filtered Total Nitrogen.....	42
Figure 5.13: Fmax for Identified PARAFAC Components 1, 2, and 3	44
Figure 5.14: Comparison of Influent EEM and Gathering Pond EEM (Sites A-D).....	47
Figure 5.15: Visually Identified C and T Peak Intensities.....	48
Figure 5.16: T Peak Intensity over Established Baseline	49
Figure 5.17: Correlation Coefficient (<i>r</i>) for all Parameters of Interest.....	51

Figure 5.18: Correlation Coefficient (r) for Pre-Bloom, Bloom Growth, and Bloom Decline 54

List of Tables

Table 2.1: Commonly Identified Fluorophores ¹	16
Table 2.2: PARAFAC Components Identified in Algal Impacted Waters	18
Table 5.1: Lateral Canal Ortho-P Investigation	40
Table 5.2: PARAFAC Identified Fluorescent Components within the Milford Gathering Pond.	46
Table 5.3: Correlations (r^2) for Parameters of Interest	51
Table 5.4: Correlations (r^2) for Pre-Bloom, Growth, and Decline Phases	53

Acknowledgements

I would like to express my deep gratitude to my academic supervisor Prathap Parameswaran for providing me with the opportunity to undertake this master's thesis and for his continuous support throughout my time at Kansas State University. I would also like to thank all my friends and fellow researchers in Fielder 0082, Kahao Lim, Chris Chiu, Arvind Kannan, Evan Heronemus, and Priyasha Fernando for not only helping me with my research, but also making my time at K-State so memorable.

This research was funded by National Science Foundation Grant #1828571 and the Fornelli Engineering Professorship.

I would also like to acknowledge Dr. Elizabeth Smith from the Kansas Department of Health and Environment and Daric Schneidewind from the Kansas Department Water, Parks, and Tourism for taking the time to meet with me, provide suggestions and improvements for my research, and share data with me. In addition, I would like to thank Dr. Leigh Terry and Melanie Vines from the University of Alabama for their help with running and validating my PARAFAC model.

I would also like to mention and thank my family who supported me throughout my entire educational journey; especially my dad, Rob Randig, and grandfather, Bob Randig, for inspiring me to become an engineer and always supporting me.

Chapter 1 - Introduction

Background

Freshwater harmful algal blooms (FHABs) are a rapid and massive proliferations of algae or algae-like organisms that create health hazards for humans and/or animals or cause deterioration of water quality or aesthetic/recreational value (Hudnell, 2010; Lopez et al., 2008). Effective management of algal blooms depends on the development of early warning systems that can accurately monitor cell density and toxic compounds (Richardson et al., 2010; McQuaid et al., 2011). However, management and prediction of blooms is challenging due to the complex nature of nutrient transport and hydrodynamic factors that influence bloom development (Thompson et al., 2008; Anderson, 2009). In situ fluorometers have been proposed for their potential to provide early warning of bloom development through the analysis of fluorescence signatures (Ye et al., 2011; Wang et al., 2020).

Fluorescence excitation emission matrix (EEM) spectroscopy is a useful tool to rapidly characterize organic matter (OM) in surface water (Coble, 1996). EEMs provide a visualization of water chemistry through the production of 3-D plots of fluorescence excitation wavelength, emission wavelength, and intensity on a relative optical scale (Hudson et al., 2007). During bloom events, dissolved organic matter (DOM) changes as algal cells rapidly replicate in the growth phase (H. W. Paerl, 1988; Merel et al., 2013). However, few studies have investigated the change in fluorescent DOM throughout a complete algal bloom event in a natural surface water environment. An in-depth understanding of how algal fluorescence signatures change during bloom development, growth, and decline phases is needed for in-situ fluorometers to be applied and/ or developed for full scale monitoring of surface waterbodies.

In addition, the environmental, meteorologic, and water quality parameters affecting bloom events should be examined in relation to EEM data to corroborate the bloom cycles and allow for investigation into correlations between fluorescent signatures and chemical and physical parameters.

Research Objectives

This research project aims to improve the understanding of variability of the fluorescent signatures of a complete algal bloom event with intensive monitoring in order to enhance the understanding of the application of fluorometers as a detection and monitoring tool. To accomplish this, the following objectives were set:

- To monitor the changes in fluorescent signatures of a complete bloom event in a surface water body
- To examine the fluorescent signatures in relation to environmental, meteorologic, and other water quality parameters of interest

Chapter 2 - Literature Review

Freshwater Harmful Algal Blooms

What are Algal Blooms?

When describing algal blooms, the term algae is used as an umbrella term to describe aquatic, photosynthetic organisms that are made up of true algae and cyanobacteria. Algae can be unicellular or multicellular organisms that contain chlorophyll or other pigments for photosynthesis, which convert light energy from the sun into chemical energy. When conditions are favorable for algae growth, the concentration of algae increases, and this excessive growth causes algal blooms (Ramadan, 2000; Klemas, 2012). The duration and growth of an algal bloom are dependent on environmental factors such as light, temperature, and nutrient availability (Anderson et al., 2002; Singh & Singh, 2015; Rao et al., 2019). Algal blooms can produce discoloration in water that can appear as foam, clotted mats, paint-like slicks, and scums of a variety of colors including light to dark green, yellow, red, or brown (Gatz, 2019).



Figure 2.1: Algal Paint-like Slicks and Scums Observed in the Milford Gathering Pond

Algal blooms are considered harmful algal blooms or HABs when they pose a threat to human health, aquatic ecosystem health, and potentially cause economic damage.

Factors Contributing to Blooms

Nitrogen (N) and phosphorus (P) are the most widely studied nutrients in relation to algal blooms because they are the primary nutrients that limit algal growth. Nitrogen occurs in water in several dissolved forms including nitrate, nitrite, and ammonium. Algae convert these forms of nitrogen to ammonium before using it for biomass production (Yao et al., 2020). Phosphorous, like nitrogen, is a critical nutrient required for all forms of life. The most common form of phosphorous used biologically is phosphate or $\text{PO}_4\text{-P}$. Phosphate is used in DNA synthesis, in carriers like adenosine triphosphate (ATP) used for the creation and movement of cellular energy, and serves as a building block for cell membranes (Anderson et al., 2002).

Additional micronutrients that affect algal blooms include silicon, iron, potassium, calcium, and magnesium. Silicon is required in the creation of cell walls in diatomic algae (Anderson et al., 2002). Iron is an essential mineral in algal growth and plays a role in photosynthesis, respiration, nitrogen fixation, and protein and nucleic acid synthesis (Kong et al., 2014). Recently, vitamins have also been found to be important in algae growth. Vitamin B_{12} is essential for the synthesis of amino acids, deoxyribose, and the reduction and transfer of single carbon fragments in many biochemical pathways (Tang et al., 2010). In addition, vitamin B_1 (thiamine) plays a pivotal role in intermediary carbon metabolism and is a cofactor for number of enzymes involved in primary carbohydrate and branched-chain amino acid metabolism (Tang et al., 2010).

There are many natural and anthropogenic sources of nutrients that can stimulate a bloom, including sewage, animal waste, atmospheric deposition, ground water inflow, and agriculture and other fertilizer runoff (Anderson et al., 2002; Hudnell, 2010).

Fertilizer Runoff

Excess fertilizer applied to crops and fields contributes to increased nitrogen and phosphorus entering water bodies during rainfall events (Gatz, 2019). Fertilizer use has been steadily increasing since the 1950s. There has also been a shift in the chemistry of nitrogenous fertilizers used in agriculture. Ammonium was historically preferred, but urea is now prominently used due to its high yield relative to cost and safety (H. W. Paerl et al., 2016). Urea rapidly hydrolyzes to NH_4^+ in water, which is an important form of nitrogen used by algae (Shumway et al., 2018). 80% of nitrogen and 25-75% of phosphorus fertilizers are lost from the fields where they are applied and enter surface water through runoff and infiltration and groundwater through leaching (Wurtsbaugh et al., 2019; H. W. Paerl & Barnard, 2020). Nitrogen and phosphorus are two of the three major ingredients in fertilizers; therefore, agricultural runoff is the main contributor of these nutrients in aquatic ecosystems.

Animal Feeding Operations (AFOs)

Livestock and poultry production in the U.S. is primarily comprised of large operations separated from the land-based production of their feed. Animals are raised in confinement where feed is brought to the animal rather than the animals seeking feed in a pasture or range (U.S. EPA, 2013). These practices have caused large, confined animal feeding operations (CAFOs) to produce large volumes of manure over small areas of land. The high concentrations of waste per unit area lead to concentrations of manure that exceed the beneficial needs of the farmland where it was produced and commonly cause the contamination of adjacent waters (Shumway et al., 2018; U.S. EPA, 2004). A 2007 USDA report found that 60 to 70 percent of the manure's nitrogen and phosphorus may not be able to be assimilated by the farmland in which it was generated (Vilsack & Clark, 2009). In addition, dairy and swine manure is often stored in lagoons and applied to land

as a liquid, which increases the nutrient mobility into the environment (Sands & Wood, 2019). Nitrogen and phosphorus from these lagoons enter the environment through overland discharge and from leachate into groundwater.

Wastewater Pollution

Municipal wastewater treatment plants process wastewater from residential homes and commercial and industrial businesses. The treated wastewater contains nitrogen and phosphorus from human waste, food, and phosphate containing soaps and detergents (Gatz, 2019). Failing septic systems are another source of wastewater pollution. When septic systems are improperly managed, nitrogen and phosphorus can be released into local water bodies or groundwater (*Nutrient Pollution: Sources and Solutions*, 2015). Septic systems often fail due to aging, poor design, overloading the system, and poor maintenance (Gatz, 2019).

Recovering nitrogen and phosphorus from wastewater is an emerging technique being researched and implemented in wastewater treatment facilities. The rationale is two-fold; first, recovery systems will keep nutrients from reaching surface water bodies, and second, recycling and reusing these nutrients will sustainably meet nutrient demands (Shaddel et al 2019). However, this advanced treatment is still a novel technology and has been implemented in very few treatment plants in North America (Wurtsbaugh et al., 2019). Implementing closed loop sustainable practices will help to improve water quality and potentially decrease the occurrence of algal blooms.

Atmospheric Deposition of Nutrients

Atmospheric deposition has been shown to be significant source of nitrogen into aquatic systems. Atmospheric deposition refers to the phenomenon where pollutants are deposited from the atmosphere in the form of dust or precipitation (Pacyna, 2008). Nitrogen has many gaseous forms including N_2 , N_2O , NO , NH_3 that can readily exchange with the atmosphere and be

transported on a global scale (H. W. Paerl & Barnard, 2020). Nitrogen in the atmosphere has increased due to NO_x emissions from fossil fuel burning and through volatilization of nitrogen from animal manures and other land-based fertilizer applications (Shumway et al., 2018). According to Wurtsbaugh et al., atmospheric deposition has increased threefold over land, and twofold over the oceans (2019). Atmospheric deposition of nitrogen can have significant impacts on both the local and continental scale of nutrient transport.

Hydrologic Changes

Anthropogenic activities have dramatically altered hydrologic features which in turn alter the transport mechanisms of nutrients to waterbodies (Hudnell, 2008). Increased imperviousness in watersheds, channelization of streams and rivers, and removal of native vegetation contribute to increases in the rates and qualities of nutrients transported into water bodies (Hudnell, 2008). In addition, shorter residence times reduce the ability of natural systems to biologically attenuate the nutrient loads leaving the watershed. River discharge has been affected by the construction of large dams and other consumptive uses (Graf, 1999). Fragmentation of large river systems due to dams prevent the free movement of organisms, alters temperature regimes, reduces sediment transport and alters nutrient loads and proportions in downstream waters (Shumway et al., 2018). These altered flows can create “windows of opportunity” for HABs to develop or create conditions where algae are able to proliferate.

Climate Change

Climate change is causing changes in precipitation patterns, increasing temperatures, and producing strong vertical stratification and altered wind speeds, which have all been linked to HAB magnitude, frequency, distribution and duration (Shumway et al., 2018; H. W. Paerl & Barnard, 2020). Global temperatures are increasing, a fact well accepted to be related to

anthropogenic activities (Allen et al., 2018). Temperature influences growth rate, mobility, germination, photosynthesis, and various other processes that affect the ability of algal cells to survive in a particular area (Shumway et al., 2018). In addition, storm events are becoming more extreme and have higher amounts and intensities of rainfall, and droughts are becoming more severe. This causes large changes in hydrologic variability, leading to more episodic discharge periods where high amounts of nutrients are transported in runoff events (H. Paerl, 2014; Shumway et al., 2018). Excessive amounts of runoff can also enhance vertical stratification in waters. Bloom forming algae have the ability to alter their buoyancy based on varying light and temperature (H. Paerl, 2014). These algae will position themselves at physically and chemically favorable depths and create a persistent bloom. Wildfires brought on by climate change can also lead to nutrient loading due to increased mobility of sediments, especially when followed by extensive rainfall and flooding (H. W. Paerl & Barnard, 2020).

Effects of Algal Blooms

Freshwater algal blooms have a range of impacts on human health, environmental health, and the economic value of ecosystems.

Human Health Impacts

While there are many types of algae and algae-like microorganisms that cause HABs, cyanobacteria typically cause the most frequent and severe blooms (Chapra et al., 2017). Cyanobacteria HABs produce toxins, called cyanotoxins, that can cause hepatic (liver-related), neurologic, respiratory, dermatologic, and other symptoms (H. Paerl, 2014). Humans are exposed to cyanotoxins through the consumption of tainted drinking water fish or shellfish, swimming or recreated in water with cyanotoxins, or inhaling aerosolized toxins. Cyanotoxins have been implicated in human and animal illness and deaths in at least 43 states (Graham et al., 2017).

Algal blooms also pose a threat to drinking and industrial water production (Henderson et al., 2009; Dawson, 2011). These blooms can cause water discoloration, odor and toxicity problems, and even operational problems within water treatment plants (Villacorte et al., 2015). The extent of the threat of human consumption of contaminated drinking water is not completely clear, but the EPA is currently assessing cyanotoxin occurrence in drinking water to determine if actions regarding drinking water guidance, health advisories, or regulations are necessary (Lopez et al., 2008).

Aquatic Ecosystem Health Impacts

Ecosystem impacts stemming from the effects of HABs are well documented. An overabundance of algae can block out sunlight and clog fish gills (Gatz, 2019). During prolonged blooms, the reduced light penetration to the bottom of a water body kills native aquatic vegetation (Anderson, 2009). This vegetation provides stability to bed sediments and can serve as an important food source and habitat for shellfish and fish populations (Klemas 2012, Anderson 2009). In addition, as the algae die and decompose, oxygen is consumed causing a hypoxic or low oxygen state (Anderson et al., 2002; Lopez et al., 2008; Rao et al., 2019). Low oxygen events suffocate and kill fish and bottom dwelling organisms (Wurtsbaugh et al., 2019). The food web can crash as a result of the HAB and cause starvation of consumers and their predators. In addition, cyanotoxins can accumulate in primary producers and transfer up the food web (Ferrão-Filho & Kozlowsky-Suzuki, 2011).

Economic Impacts

HABs have significant economic impacts due to their threats to human health and their negative impacts on aquaculture, recreation, and tourism (Anderson, 2009; A. R. Brown et al., 2019). HAB toxins and taste-and-odor compounds result in increased treatment costs for

drinking water facilities, and algal mats interfere with reservoir operations such as drinking water intakes and hydroelectric generation (Lopez et al., 2008). In addition, closures of recreational waterbodies to protect human health can result in revenue losses for local communities, especially during holiday weekends or planned events (Ramadan, 2000). It has been estimated that HABs have cost the U.S. economy between 1.5 and 4.8 billion dollars annually due to losses in the recreational and commercial industries and effects on drinking-source and potable water (Smith et al 2019, Hudnell 2010).

Bloom Prevention and Mitigation

There are two main actions associated with effectively managing an algal bloom: prevention and mitigation. Prevention refers to actions that can be taken to keep an algal bloom from forming, while mitigation refers to dealing with an existing bloom and taking steps to reduce its impacts (Anderson, 2009). One of the largest mechanisms to prevent algal blooms is nutrient reduction from point and nonpoint sources. Because many point sources are now well managed, current efforts focus on non-point source reductions, including runoff from agriculture and urban areas (Piehler, 2008). While prevention is the most ideal solution, it is also the most difficult as it requires widespread changes in policy and human activities and can take many years to significantly improve water quality. Extensive research has been completed focused specifically on mitigating the effects of algal blooms. There are five general treatment categories that can be used to suppress the effects of algal blooms: physical, mechanical, biological, chemical, and environmental control. Examples of each are summarized below.

Physical Control

Sediment barriers can be used at the inlets of reservoirs to reduce sediment loading. This can keep nutrients, which attach to sediment surfaces, from entering surface water bodies or

reservoirs (H. Paerl, 2018). In addition, legacy nutrients in sediment can also be removed through dredging. However, dredging presents a serious logistic challenge because sediments removed from a water body must be exported and deposited out of the drainage basin, in order to avoid sediment-associated nutrients from leaching back into the system (H. Paerl, 2014). Dredging is both a labor intensive and costly solution and it can remobilize nutrients back into the water column.

Mechanical Control

Aeration, oxygenation, or artificial mixing systems can be used to increase water flow which oxygenates the water and enhances pollutant transformation, specifically of nitrogen by microbial biofilms and uptake by plant roots (Henny et al., 2020).

Clay can be used to flocculate and settle algae. However, using high loads of clay can lead to other negative ecological side effects like siltation and secondary pollution. In addition, large amounts of clay are usually unavailable on short notice and have high transportation costs (Anderson, 2009; Li & Pan, 2013; Liu et al., 2013). Other coagulants such as moringa oleifera (MO) coagulant, PAC₃, and FeCl₃, and flocculants such as chitosan, chitosan-modified local soil/sand (MLS) materials, xanthan, and polyacrylamide, have been assessed. However, the mechanics and science behind algae coagulation and flocculation are still not comprehensively understood (Li & Pan, 2013).

Biological Control

Biomanipulation is a biological control that focuses on altering the aquatic food web to increase grazing pressure on algae. Biomanipulation approaches can include introducing fish and benthic filter feeders capable of consuming bloom causing algae (H. Paerl, 2014). The long-term

efficiency of biomanipulation may lead to dominance by ungradable or toxic strains of algae, so it must be used cautiously.

Genetic control is a form of biologic control that involves genetically engineering species and introducing them into the environment to alter the environmental tolerances, reproduction, and other processes in the undesirable species (Anderson, 2009).

Decomposing barley straw and cypress leaves have been found to reduce the abundance of algae in lakes. They have an amino acid, L-lysine, that limits algae growth. However, application of straw and cypress leaves is not a good long term management strategy (Tomasko et al., 2016).

Chemical Control

Copper sulfate pentahydrate ($\text{CuSO}_4 \cdot 5\text{H}_2\text{O}$), or bluestone is a known algicide. It is toxic to many species of algae at low concentrations and presents no health hazard to domestic water supply (Ramadan, 2000). However, copper sulfate treatment is expensive as it requires time, labor, and chemical costs. Other chemical algicides include copper chelates, endothall, and formulations containing sodium carbonate peroxyhydrate (Anderson, 2009; Zhou et al., 2013).

Environmental Control

Aquatic plants compete with algae for nutrients and light which can inhibit algae growth. In addition, some aquatic plant roots secrete antibiotics that significantly suppress algae (Zheng et al., 2019). Ecological floating beds, ecological jellyfish, and ecological membrane covering of bottom sediments was found to reduce algae concentrations and improve the survival of native aquatic plant species. Additionally, these systems improve turbidity and remove phosphorous and nitrogen (Zheng et al., 2019).

Conventional Bloom Detection and Monitoring

Different technologies are used for HAB detection and monitoring. The classic approach for detection and enumeration of algal species is through direct observation by light microscopy of live or preserved material (Sellner et al., 2003). This technique provides visual confirmation of the presence of different species of algae and allows for reasonable estimates of cell abundance. However, it is also considered tedious, time-consuming, and costly, and requires a level of experience/ expertise in algae identification (Sellner et al., 2003; Chang et al., 2012).

Cell pigments can also be used as a metric for real time monitoring of algal blooms. Intracellular photosynthetic pigments in chlorophyll containing algae or cyanobacteria are measured using fluoroscopy (Chang et al., 2012). The analysis of Chlorophyll-*a* (Chl*a*) and Phycocyanin (PC) can give an estimate of cell biomass. The evaluation of algal cell density based on pigments is faster than conventional light microscopy; however, validation through microscopy is still required as pigment only allows for a rough estimate. In addition, this technique can have many internal and external interferences including turbidity, temperature, light scattering particles, and varying cell pigment content (Beutler et al., 2002; Chang et al., 2012; Henderson et al., 2009). Interferences with pigment measurement lead to an under or overestimation of algal presence in the waterbody of interest (Zamyadi et al., 2016).

The microscopy and pigment analyses only allow for real-time monitoring and data of existing algal cells. They do not allow for any predictive measurements of changes in algal communities.

Aside from cell and pigment quantification, there are also numerous methods that have been examined for the separation and identification of algal toxins as a tool to monitor blooms. However, toxins were not a focus of this study and are therefore excluded from this review.

Principles of Fluorescence Spectroscopy for Monitoring Organic Matter

Fluorescence is a commonly used technology in water sciences to investigate the composition of dissolved organic material, or DOM, in surface water (Coble, 1996, 2007; Hudson et al., 2007). DOM is composed of heterogeneous structures and compositions that contain a variety of functional groups which can combine with organic and inorganic material (Coble, 2007). DOM is transported into aquatic ecosystems through the hydrologic cycle or created in situ through microbial activity (Hudson et al., 2007). Anthropogenic activities can also be a large source of DOM which enters surface water through direct discharge, leaching, and aerial dispersal. The composition of DOM has a significant impact on the environment it exists in and fluctuations in DOM can give insights on the status and overall health of an ecosystem as it influences light attenuation, nutrient availability, and contaminant transport (Williams et al., 2010; Nebbioso & Piccolo, 2013; Wang et al., 2020).

Fluorescence is a popular technique for water quality monitoring because it is a rapid process that requires no reagents or sample preparation for analysis. Excitation Emission Matrix (EEM) fluorescence spectroscopy, coupled with parallel factor analysis (PARAFAC), is a novel, emerging technique used to characterize organic matter in aquatic ecosystems (Stedmon & Bro, 2008a). Fluorescence spectroscopy is a technique that involves exciting molecules in a sample using a beam of light, then measuring the light emitted after passing through the sample using a fluorometer (Hudson et al., 2007). This emission is translated into an EEM, which is a 3-D plot of the fluorescence excitation, wavelength, emission wavelength and intensity on a relative optical scale, see Figure 2.2. EEMs allow for visual identification of peaks, which then indicates the composition of the sample. Specific excitation and emission wavelengths are characteristic of a particular molecular fluorophore and are summarized in Table 2.1 (Henderson et al., 2009). A

fluorophore is a fluorescent chemical compound that can re-emit light upon light excitation (Fellman et al., 2010).

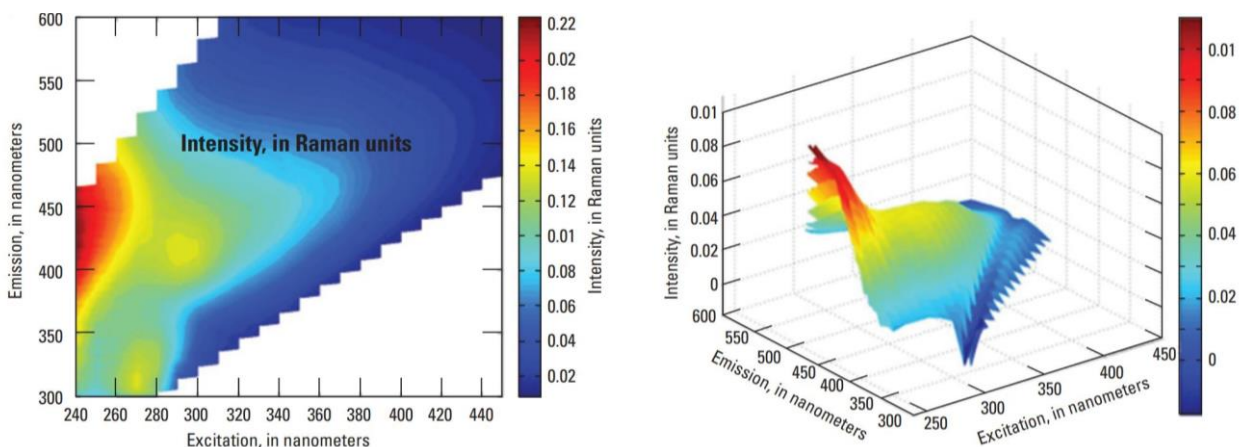


Figure 2.2: EEM Visualization (Hansen et al., 2018)

Evaluation of EEMs through Parallel Factor Analysis

Parallel factor analysis (PARAFAC) has improved peak identification by translating the fluorescence signal into individual fluorescent phenomena (Stedmon & Bro, 2008a). PARAFAC is used to decompose EEMs into their individual fluorescence components and has the ability to identify even the smallest changes in overlapping independent EEMs (Stedmon et al., 2003; Zielinski et al., 2018). Five distinct peaks (A,C,B,T, and M) are used to identify the composition and origin of DOM in EEMs (Coble, 1996; Coble et al., 1998; Coble, 2007; Hudson et al., 2007; Henderson et al., 2009). The relative locations and description of each peak are summarized in Table 2.1.

A variety of biogeochemical processes impact the nature and reactivity of organic matter in natural water systems. In naturally occurring freshwater DOM, the predominant peaks are humic (A and C) due to the breakdown of organic material in water, riparian zones, and soil (Hudson et al., 2007). Urbanization is observed through the Tryptophan material (T peaks) and Tyrosine material (B peaks). Organic matter in the aquatic systems is known to fluctuate

seasonally due to changes in flow rate and the impacts of precipitation; observed peaks reflect this change with seasonally different intensities (Stedmon & Markager, 2005a).

Table 2.1: Commonly Identified Fluorophores¹

Fluorophore	Component	λ (nm)	
		Excitation	Emission
A	Humic-like	237–260	400–500
C1	Humic-like	300–340	400–430
C2	Humic-like	370–390	460–480
M	Marine Humic-like	280–312	370–420
B1	Tyrosine-like	225–237	309–321
B2	Tyrosine-like	275	310
T1	Tryptophan-like	275	340
T2	Tryptophan-like	225–237	340–381

¹(Coble, 1996; Coble et al., 1998; Coble, 2007; Hudson et al., 2007; Henderson et al., 2009; Fellman et al., 2010)

Fluorescence spectroscopy and PARAFAC analysis have been applied to algae impacted surface water. In eutrophic surface water, a large portion of DOM can be produced as a result of the bloom and associated microbial activity which is then reflected on EEMs (Ye et al., 2011; Wang et al., 2020; Henderson et al., 2008). Previous works have shown similarities in peaks observed in relation to algal activity and are summarized in Table 2.2. The most common peaks observed are Peak A, Peak C, Peak B, and Peak T. These works have also shown changes in the fluorescence peaks throughout different phases of cell growth and decay. Henderson et al. (2008) found that tryptophan peaks dominated in the exponential phase for *Microcystis aeruginosa* and *Asterionella Formosa*, while tryptophan, tyrosine, and humic like peaks dominated during the exponential phase for *Chlorella vulgaris*. Villacorte et al. (2015) found that humic like fluorescence is microbially derived and was observed for cyanobacterial and other phytoplankton cultures. Xu et al. (2013) found that tryptophan-like fluorescence was positively correlated with *Microcystis* growth and both tryptophan-like and humic-like fluorescence were associated with

M. aeruginosa growth. In addition, Ziegmann et al. (2010) found correlations between tryptophan-like fluorescence of *M. aeruginosa* and Chl-a and toxin concentrations.

Table 2.2: PARAFAC Components Identified in Algal Impacted Waters

Paper Title	# of Components Identified	Location of Excitation and Emission Maxima	Typical Peak Classification
Characteristics of Dissolved Organic Matter and Its Role in Lake Eutrophication at the Early Stage of Algal Blooms - A Case Study of Lake Taihu, China (Wang et al., 2020)	3	224 (276) : 316	Peak B
		232 (296) : 348	Peak T
		260 (340) : 450	Peak C
Fluorescence descriptors for algal organic matter and microalgae disintegration during ultrasonication (Khan et al., 2022)	3	280 : 310	Peak T
		225 (275) : 310-314	Peak B
		245 (365) : 400	Peak C
Insights into extracellular polymeric substances of cyanobacterium <i>Microcystis aeruginosa</i> using fractionation procedure and parallel factor analysis (Xu et al., 2013)	4	220 : 340	Peak T
		280 : 340	Peak T
		200 (220, 270) : 296	Peak B
		250 (340) : 438	Peak C
Emerging role of dissolved organic nitrogen in supporting algal bloom persistence in Lake Taihu, China: Emphasis on internal transformations (Yao et al., 2020)	4	240 : 420	Peak C
		280 : 340	Peak T
		270 : 300	Peak B1
		275 : 308	Peak B2
Characterisation of algal organic matter produced by bloom-forming marine and freshwater algae (Villacorte et al., 2015)	5	330-350 : 420-480	Peak C1
		250-260 : 380-480	Peak C2
		300-330 : 380-420	Peak M
		270-280 : 300-320	Peak B
		270-280 : 320-350	Peak T
Fluorescence spectroscopic characterisation of algal organic matter: towards improved in situ fluorometer development (Khan et al., 2019)	6	<250 (335) : 438	Peak A
		<255 (355) : 475	Peak C
		<250 (290) : 345	Peak T1
		<250 (300) : 390	Peak A
		260 : 304	Composite Peak B and T
		265 : 354	Peak T2

Paper Title	# of Components Identified	Location of Excitation and Emission Maxima	Typical Peak Classification
Tracing the production and degradation of autochthonous fractions of dissolved organic matter by fluorescence analysis (Stedmon & Markager, 2005b)	7	<240 (355) : 476	Peak A
		<240 (340) : 398	Peak A
		295 : 398	Peak M
		275 : 306 (338)	Peak T
		345 :434	Peak C
		280 : 338	Peak B
		420 (275) : 488	No Peak

Inferences and Knowledge Gaps

There is an urgent need for monitoring techniques that are able to sensitively detect and qualify algal biomass in a short period of time for bloom management. The key to effective bloom management is early warning systems that allow for the timely implementation of mechanisms for bloom control. Current practices for bloom monitoring include cell and pigment enumeration, however, these technologies do not provide any predictive indicators. Fluorescence spectroscopy is a powerful tool to analyze and characterize surface water and has the potential for incorporation into an online monitoring system. Fluorescence spectroscopy has been investigated as a tool to monitor recycled water systems (Henderson et al., 2009) and drinking water treatment (Shutova et al., 2014), and prediction of membrane fouling (Bergman et al., 2020; Lim et al., 2020). The application of fluorescence spectroscopy for monitoring of a complete algal bloom event with intensive sampling is needed to further evaluate this technology, and the following knowledge gaps need to be addressed:

- Studies investigating changes in fluorophores during algal growth phases have been completed in lab scale experiments, however no in-depth intensive monitoring has been completed in a natural surface water system.
- The impact of environmental and meteorologic conditions on bloom development is well documented but needs to be considered in tandem with the fluorophores identified using fluorescence spectroscopy.

Chapter 3 - The Milford Gathering Pond

The study was conducted at the Milford Gathering Pond located in Geary County, KS and is located 400 meters downstream from the Milford Lake dam, see Figure 3.1.

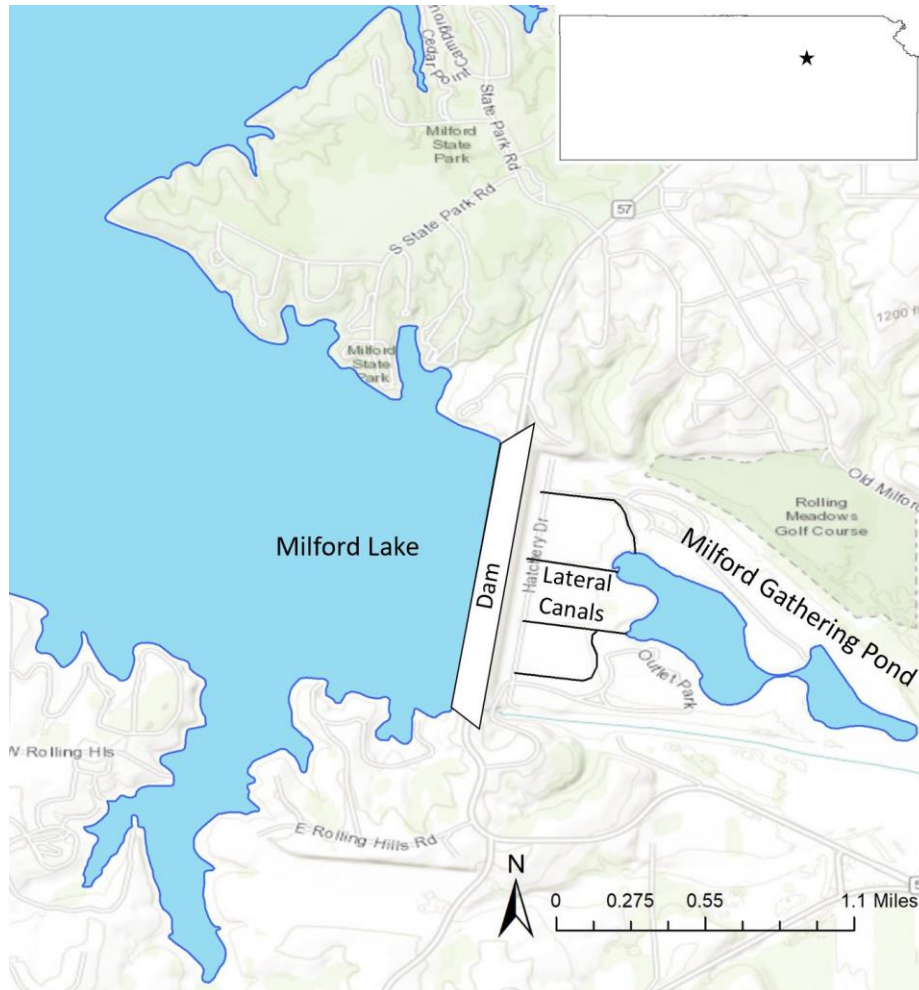


Figure 3.1: Location Map of Milford Lake and the Milford Gathering Pond

The Milford Lake dam was constructed by the U.S. Army Corps of Engineers and was completed in 1966. The site conditions of the dam are unique because the dam was built on an alluvial aquifer rather than a thick blanket of silt and clay, which is most common for earthen dams (Stark et al., 2011). As a result, the dam is more permeable than other dams, and the seepage velocity of water flowing under the dam is greater (Huggins & Howick, 1998). A cross section of the dam is detailed in Figure 3.2.

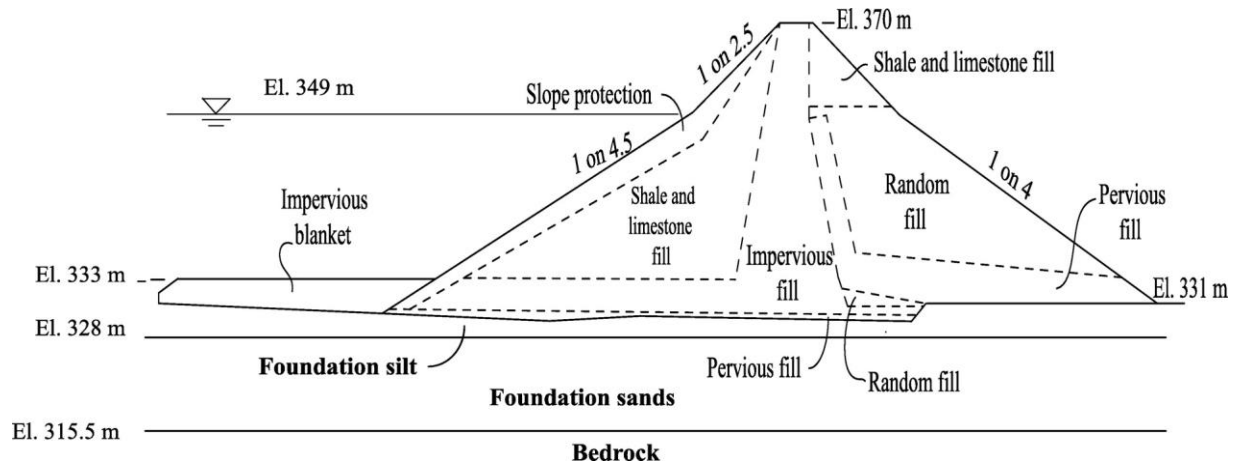


Figure 3.2: Milford Dam Cross Section (Stark et al., 2011)

The water draining from the dam is collected by 73 pressure relief or weep wells and conveyed in four lateral canals to the Milford Gathering Pond. In addition to the water from the weep wells, the Gathering Pond also received direct seepage from the aquifer below Milford Lake and the Republican River. The alluvial deposits consist of a natural fine-grained soil blanket that is underlain by sand deposits and have a thickness that ranges between 14 and 17 meters (Stark et al., 2011). The alluvium is saturated and the groundwater surface near the downstream toe of the dam is about 1.2m below the ground surface. It is estimated that 50% of the input to the Gathering Pond is from the lateral canals carrying the dam seepage and 50% is direct seepage from groundwater (Huggins & Howick, 1998). The Gathering Pond has a total volume of $8 \times 10^7 m^3$, a water residence time of 35 days, and a maximum depth of 3.8 m.

The Gathering Pond is used as a source water for the Kansas Department of Wildlife, Parks, and Tourism, Milford Fish Hatchery. During its first year of production in 1985, the hatchery encountered disease, poor growth, and excessive mortality (Huggins & Howick, 1998). An investigation concluded that poor water quality was the cause of the poor fish production. One of the water quality concerns was the eutrophic condition of the Gathering Pond. The eutrophic condition was attributed the high nutrient concentrations from groundwater seepage

through Milford Dam. Nutrient concentrations below the dam were much higher than above it, and a plume of elevated nutrients appeared to emanate from the center of the dam (Huggins & Howick, 1998).

Since the eutrophic conditions were first recorded in 1985, yearly algal blooms have plagued the Milford Gathering Pond. The current hatchery manager, Daric Schneidewind, noted that they have grown in severity and duration over his career. The Kansas Department of Health and Environment (KDHE) has recorded and confirmed algal blooms at the Gathering Pond in 2019, 2020, and 2021. However, KDHE only samples and confirms HAB events based on a complaint-based response program. The timings for the KDHE-established watch and warning during 2021 are detailed in Figure 3.3. A watch indicates a harmful algal bloom is possible and may be present, while a warning indicates a harmful algal bloom is expected or present. During the warning period, the Milford Gathering Pond was closed to the public due to the health hazards to both people and their pets.

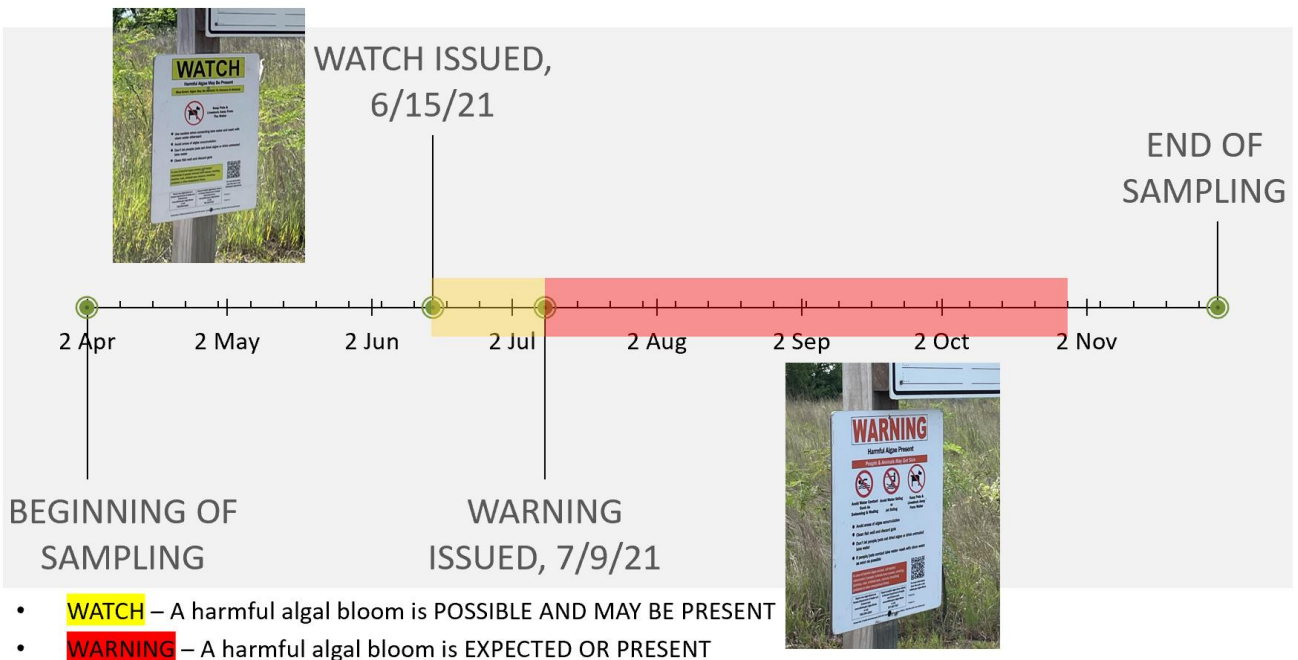


Figure 3.3: Timeline of KDHE Established HAB Watch and Warning in the Milford Gathering Pond

KDHE measures cell count and toxin concentration as part of their HAB Response Program. Samples at the Gathering Pond were taken on June 28th, August 2nd and 26th, and September 20th, 2021. The results show that cyanobacteria (Microcystis and Other Cyanobacteria) dominate within the Gathering Pond with microcystin concentrations ranging from 1.3 - 2.6 µg/L.

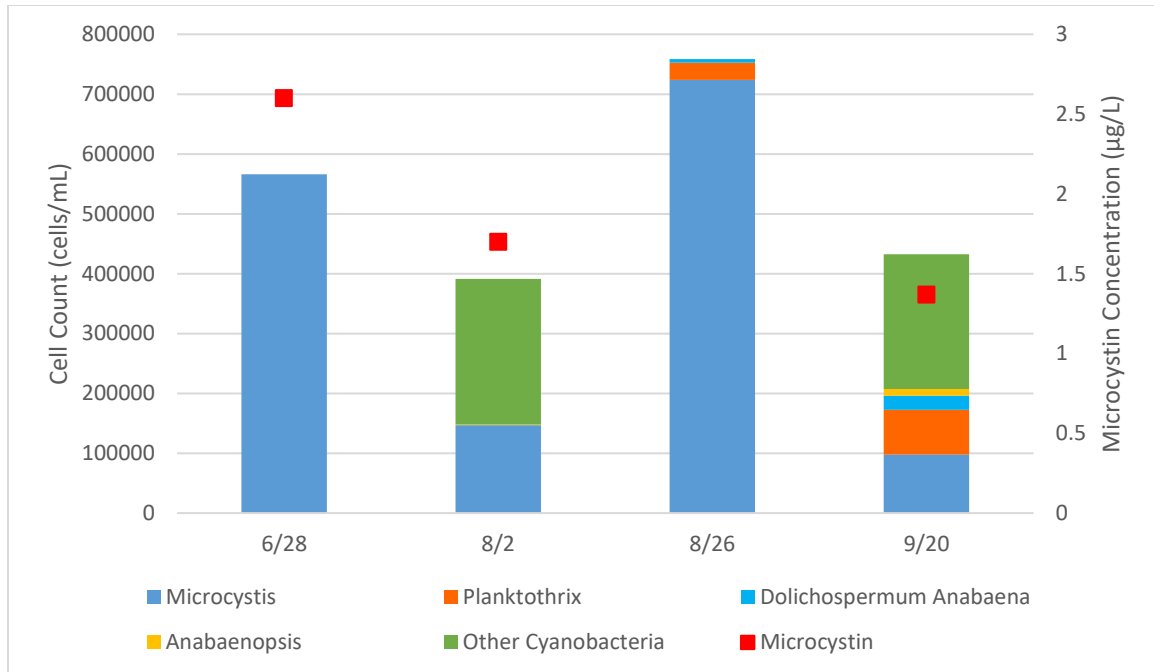


Figure 3.4: KDHE HAB Response Program Sampling Data for the Milford Gathering Pond in 2021

The Milford Gathering Pond was considered an optimal site for this research study because it experiences yearly severe harmful algal blooms, is currently sampled and monitored by the Kansas Department of Health and Environment, and its small size allows for sampling at the influent into the pond and at various representative locations throughout the pond.

Chapter 4 - Materials and Methods

Sample Collection

The Milford Gathering Pond was studied for an eight-month period during April 2021 – November 2021 to ensure sampling captured the entirety of the harmful algal bloom event. Biweekly samples were collected at five locations around the pond with a total of 206 samples collected; Figure 4.1 details the locations of the five sampling locations around the pond.



Figure 4.1: Sampling Site Location Map

Sites A and C are located in shallow areas (depth < 0.5 meters) and Sites B and D are located in deeper areas (depth > 1 meter). Water samples for Sites A - D were collected at a minimum of 0.25 meters below the water surface. Influent water samples were collected in the northern most lateral canal that carries water from the pressure relief wells into the Gathering

Pond. Panoramic pictures of each site are detailed in Figure 4.2. All samples were collected in sterile 30mL polypropylene test tubes and transported in a cooler. Once in the laboratory, samples were filtered through 1.5 μm Cole-Parmer nylon filters to remove any particles that may cause light scatter and interference with fluorescence measurements (Cole-Parmer #EW-32819-12, IL, USA). Samples were analyzed for temperature, turbidity, pH, orthophosphate, total carbon, total nitrogen, and fluorescence spectroscopy within 48 hours of collection.

Site A



Site B



Site C



Site D



Influent



Figure 4.2: Panoramic Pictures of Sampling Sites

Meteorologic Data Collection

Meteorologic data for the area around the Milford Gathering Pond was accessed from the Manhattan weather station and available through the Kansas Mesonet Historical Weather Data (*Kansas Mesonet*, 2021). The Manhattan weather station was selected due to its proximity (< 20 km) to the Gathering Pond. Parameters relating to HAB events investigated were precipitation, air temperature, average wind speed at 2 meters, and solar radiation.

Measurements of Temperature, pH, Turbidity, Orthophosphate, Total Carbon, and Total Nitrogen

Temperature (°C), pH, and turbidity (NTU) were measured in triplicates in the field. Temperature was measured with the YSI Pro 10 pH Meter using the temperature reading on the multiparameter interface (Xylem Inc., OH, USA); pH was measured with the Thermo Scientific Orion 3-Star pH Meter (Thermo Fisher Scientific Inc., MA, USA); and Turbidity was measured with a HACH 2100Q Portable Turbidimeter (Hach, CO, USA). Concentrations of Orthophosphate (mg PO₄-P/L), total filtered carbon (mg C/L), and total filtered nitrogen (mg N/L) were measured in a laboratory setting. Orthophosphate was measured with either the HACH Low Range Phosphorus TNTplus Vial Test or the PhosVer® 3 Ascorbic Acid Test 'N Tube™ HACH Method 8048 and a Hach Spectrophotometer (Hach DR3900, CO, USA). Filtered total carbon and filtered total nitrogen were measured using the Shimadzu TOC-L CSH Total Organic Carbon Analyzer (Shimadzu Corp., Kyoto, Japan).

Fluorescence EEM-PARAFAC Analysis

Fluorescence excitation-emission matrices (EEMs) were produced using a 1 cm path length quartz cuvette (Starna, Australia) and a Horiba Aqualog spectrometer (Horiba, Kyoto,

Japan). Filtered samples were scanned at excitation wavelengths ranging from 240 to 600 nm with a 3 nm increment and emission wavelengths ranging from 212.96 to 622.67 nm with a 3.28 nm increment. Raman scans were obtained at an excitation wavelength of 350nm over an emission range of 212.96 – 622.67 nm and were used for EEM spectra normalization.

Raw spectral data was corrected using instrument specific excitation and emission factors, Raman normalization, and blank subtraction (Lawaetz & Stedmon, 2009; Cory et al., 2010; Murphy et al., 2010). First and second order Rayleigh scattering peaks and Raman scattering peaks were removed before PARAFAC analysis (Zepp et al., 2004; Stedmon & Bro, 2008b; Murphy et al., 2013).

PARAFAC analysis was performed in MatLab (R2020a) using the drEEM toolbox (Version 0.5.0) to mathematically and statistically deconvolute the EEM data collected into its DOM components (Murphy et al., 2013). A total of 206 EEM spectra were analyzed (42 Site A, 42 Site B, 42 Site C, 42 Site D, and 38 Influent). Outlier samples (n = 15) were excluded from the dataset using outlier tests and leverage plots. The outlier test selection and removal of samples was completed following the PARAFAC tutorial (Murphy et al., 2013). The final leverages and loading are detailed in Figure 4.3. A complete list of outliers is available in Appendix A.

Half-split validation was used to validate the EEM-PARAFAC model with Tucker correlation coefficient > 0.95 (Murphy et al., 2013). The final PARAFAC model had three components: Component 1 (C1), Component 2 (C2), and Component 3 (C3).

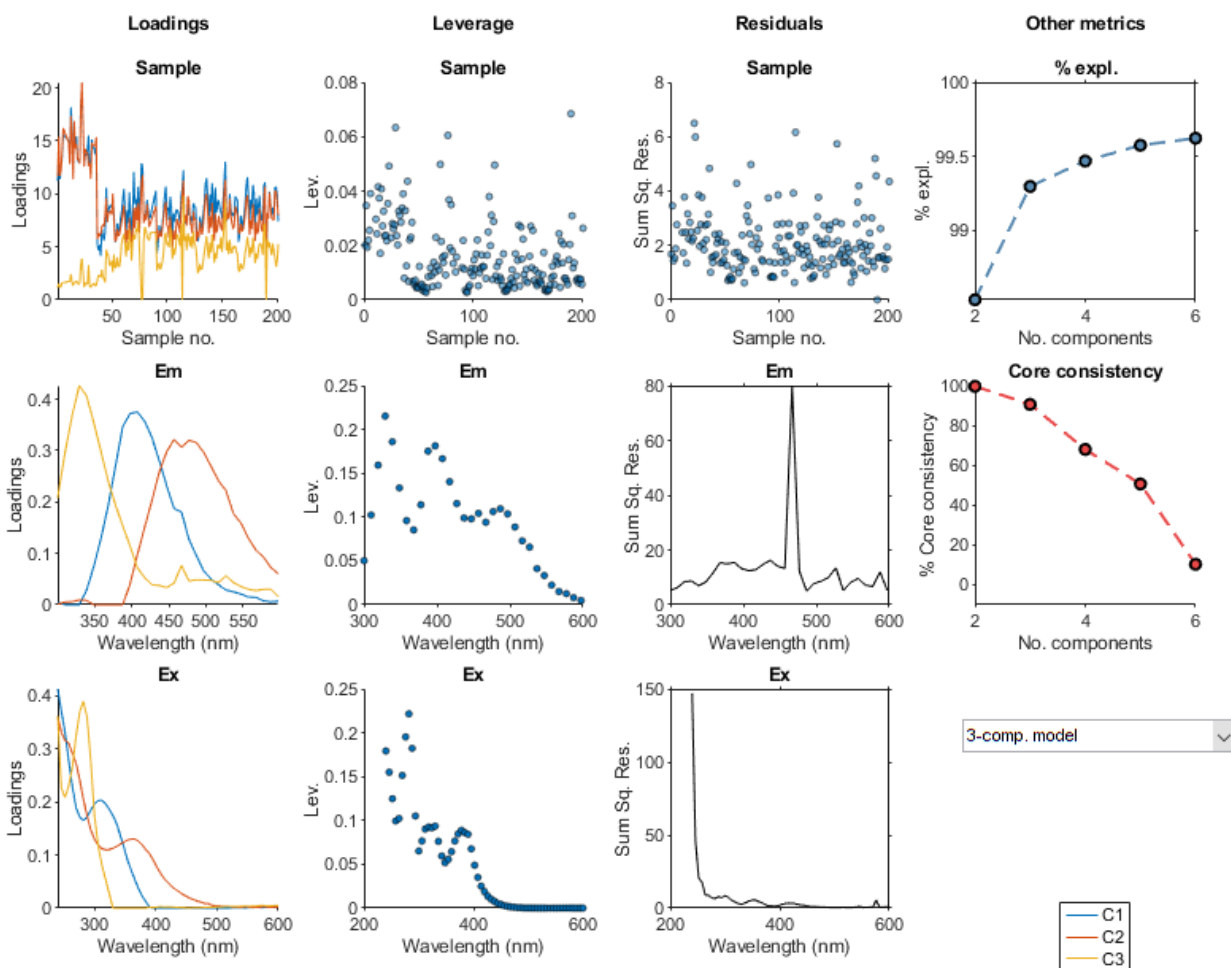


Figure 4.3: PARAFAC 3 Component Model Leverages and Loadings

The PARAFAC model was also validated through comparison with other identified PARAFAC components on OpenFluor. OpenFluor is an online spectral library of organic fluorescence spectra (Murphy et al., 2014). A total of 43 matches were found for component 1, 42 matches for component 2, and 14 matches for component 3 with a confidence level of 0.98. Graphs of the matches and derived fluorescence loadings are detailed in Figure 4.4.

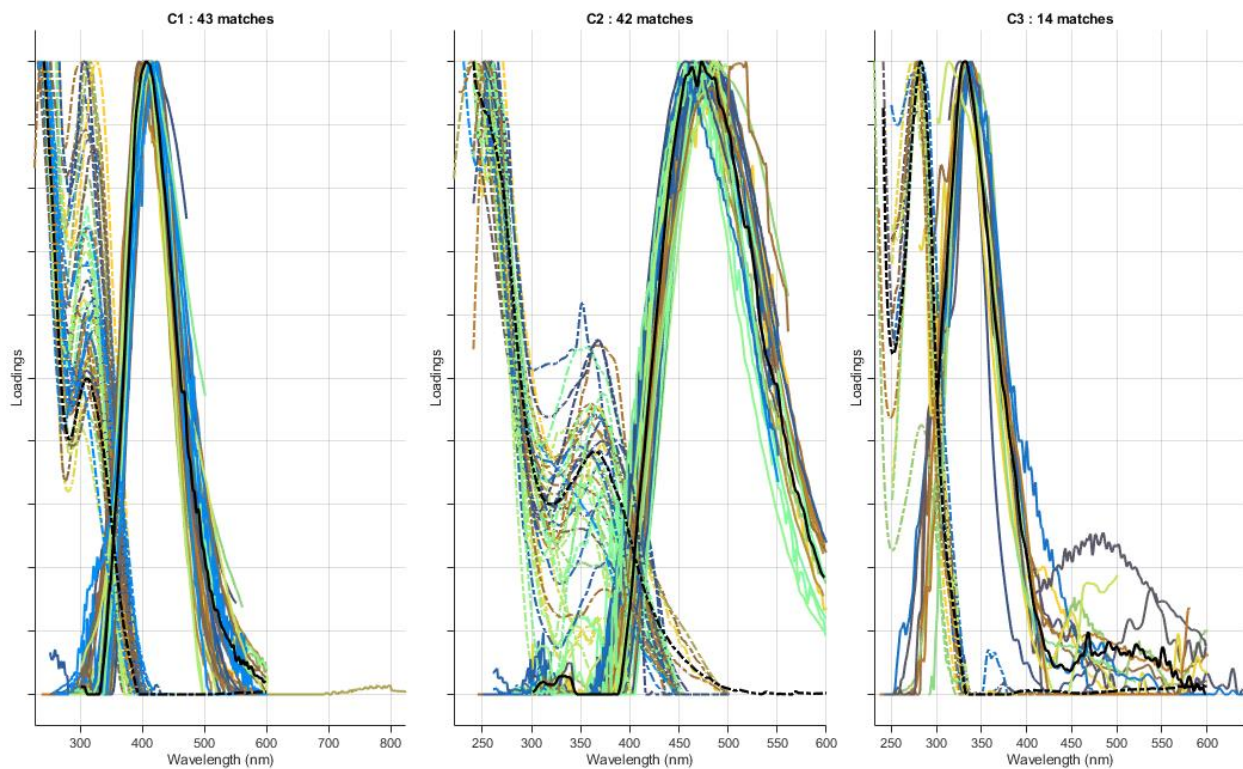


Figure 4.4: OpenFluor PARAFAC Component Matches

The maximum fluorescence intensity, F_{\max} , was derived through the PARAFAC model and represents the relative concentration or intensity of each PARAFAC component. In addition, visual peak identification was performed on the corrected EEMs, and the peak intensities were recorded.

Chapter 5 - Results and Discussion

Meteorologic and Environmental Conditions

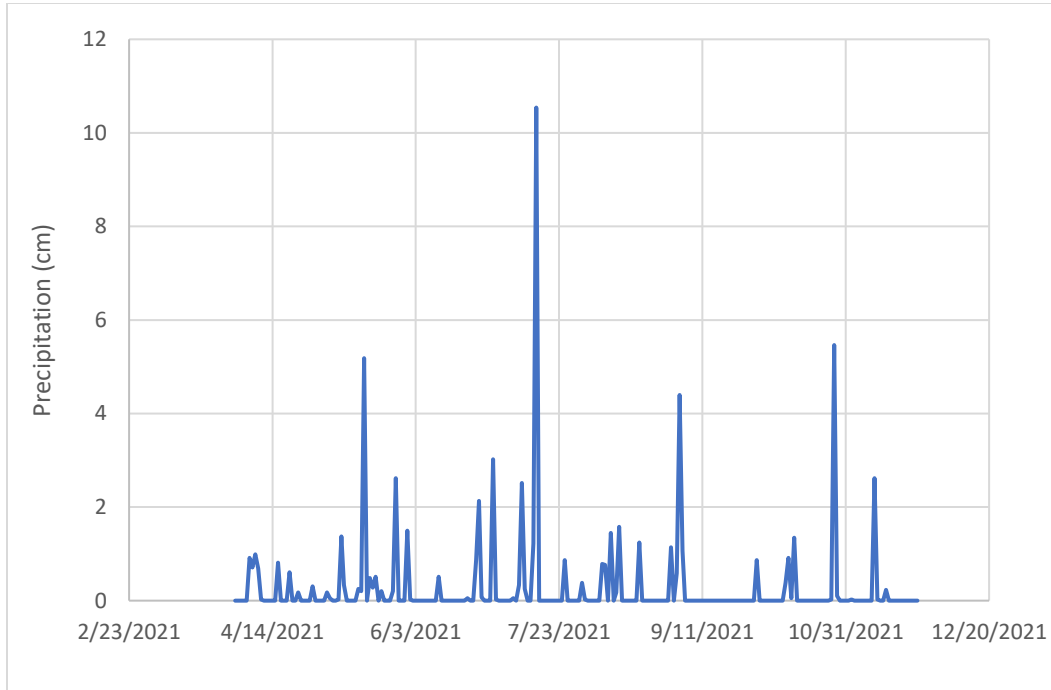


Figure 5.1: Precipitation Data

Precipitation events are known to increase HABs through the generation of nutrient rich runoff (H. W. Paerl et al., 2011). However due to the nature of inflows to the Gathering Pond being from groundwater and relief well seepage, direct precipitation or its anticipated runoff are not thought to be major contributions of nutrients for the study location. On the contrary, precipitation events have the potential to dilute algal biomass concentration and cause washout, so, it is important to note in relation to turbidity measurements (Ballah et al., 2019). The largest recorded rainfall event during sampling was on July 15th with a cumulative total of 10.5 cm, see Figure 5.1. A decrease in turbidity was observed after the rainfall event which corroborates the above statement.

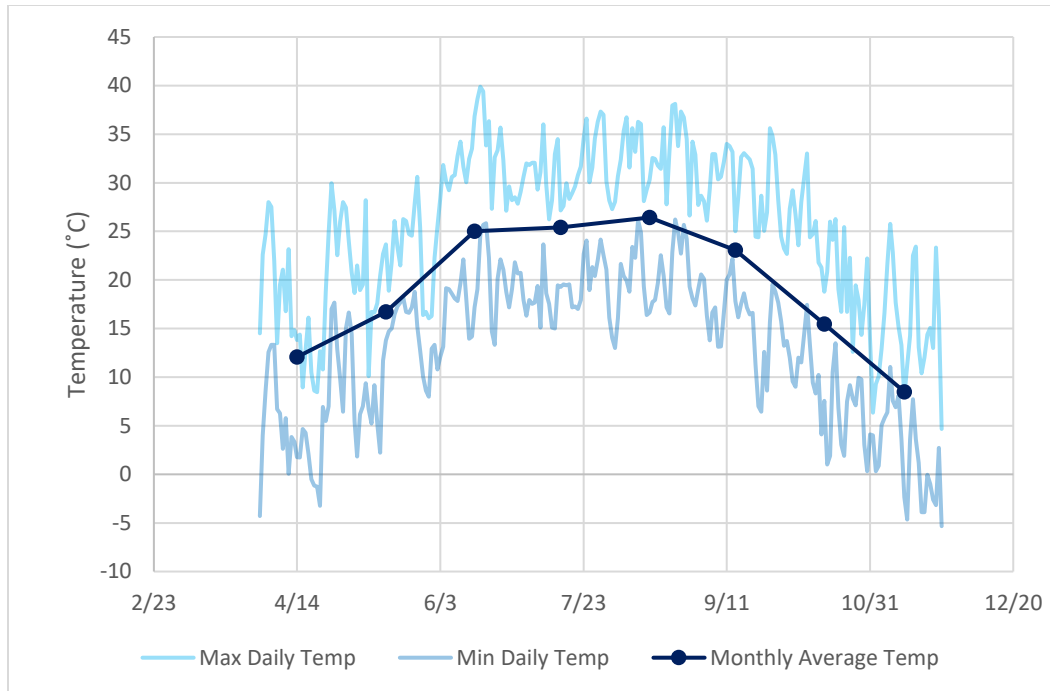


Figure 5.2: Air Temperature Data

Increased water temperatures favor harmful algal blooms through increased vertical stratification, reduced vertical mixing, and increased internal phosphorus loading from sediments (Ho & Michalak, 2020; H. W. Paerl & Huisman, 2008). Warm temperatures were recorded into September and October that allowed the bloom to persist well into the Fall, see Figure 5.2.

Wind speed influences HABs by increasing mixing within the water column (Anderson et al., 2002). High winds can push algal communities into small areas of intense accumulation (Ballah et al., 2019). The Gathering Pond generally experiences wind from the South-Southeast direction in the months from April to September, and wind from the South-Southwest direction in October and November. This indicates that algal biomass was primarily being pushed towards Sites B and C. A large accumulation of algal scum was observed at Site B on June 3rd, see Figure 5.3. These large accumulations continued to be observed throughout the remainder of the study period.



Figure 5.3: Algal Scum Accumulation Observed on June 3rd at Site B

Mean daily wind speeds increased towards the end of sampling in late October and early November, which is typical for this geographic location, as indicated in Figure 5.4.

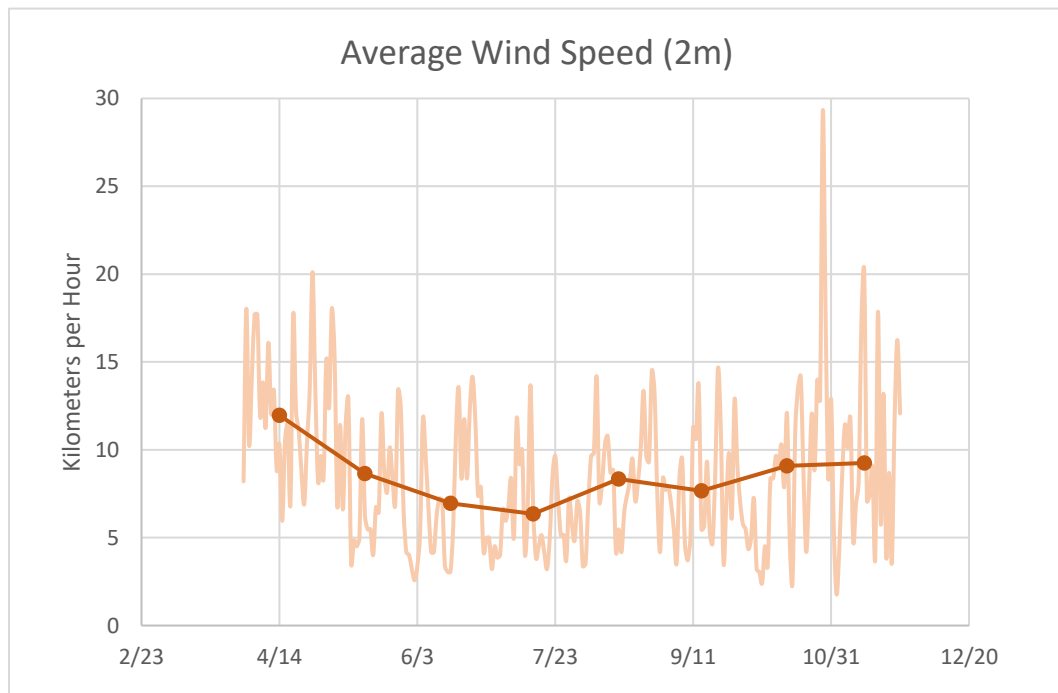


Figure 5.4: Mean Daily Wind Speed at 2m

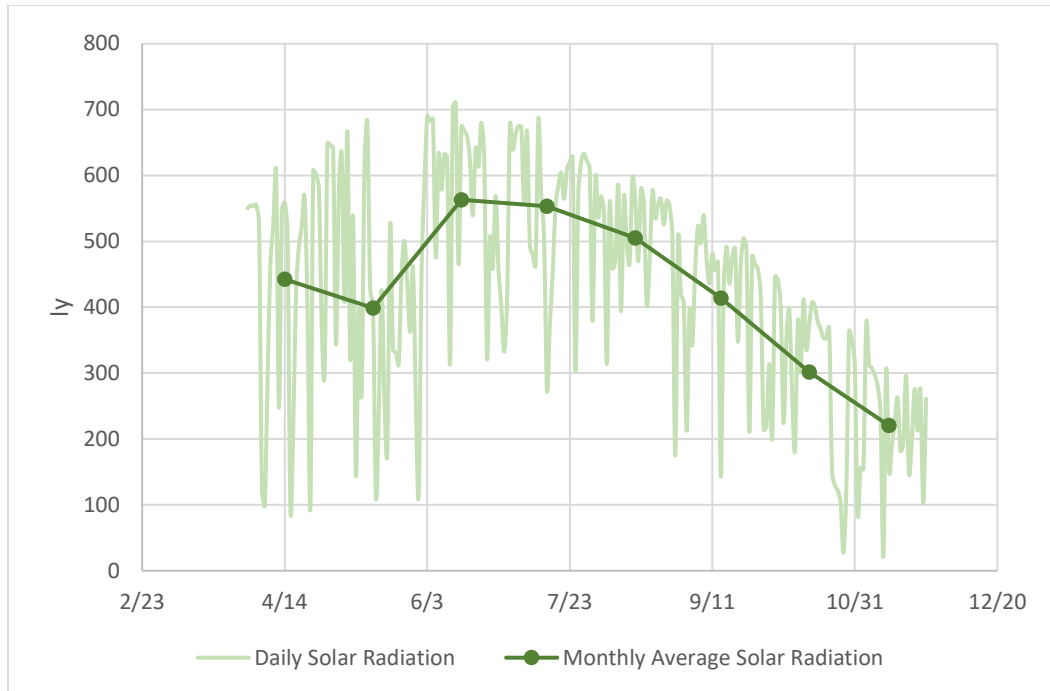


Figure 5.5: Solar Radiation Data

Solar irradiation or light is a limiting resource for algal growth (Molinari et al., 2021).

The assimilation of nutrients through photosynthesis by algae is dependent on light (Anderson et al., 2002). Solar radiation was highest during June and decreased each month until sampling ended in November, see Figure 5.5.

Water Quality Parameters

Turbidity

For the purposes of this study, turbidity is used as a general indicator of algal biomass in the Milford Gathering Pond. Previous works have identified turbidity as an effective measurement of algal density and productivity (R. Brown, 1984; Ferrando, Noelia F. et al., 2015; Molinari et al., 2021). However, because turbidity is the measure of light scattering and absorption caused by the presence of suspended particles in a fluid, it also captures inorganic (silts or clay) and organic (phytoplankton or zooplankton) particles (Brezonik et al., 2019). Therefore, measurements can be influenced by mixing within the water column or large

precipitation events. Figure 5.6 shows an example of turbidity within the Milford Gathering Pond at the beginning of the bloom event.

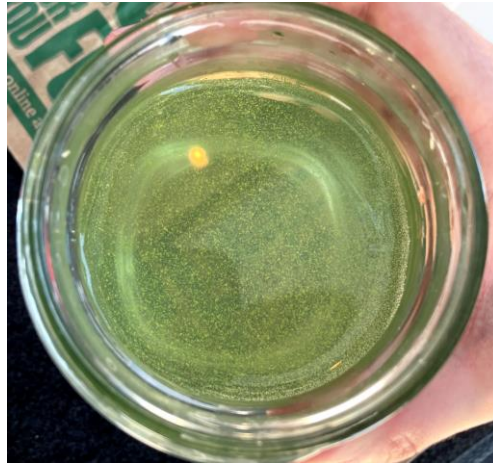


Figure 5.6: Visual Example of Turbidity within the Gathering Pond on June 15th

A large rainfall event (10.5 cm) on July 15th was shown to decrease turbidity. It took about two weeks for the turbidity to recover to pre-rainfall measurements, see Figure 5.7. This corroborates previous findings that suggested a decrease in turbidity due to dilution and washout associated with rainfall.

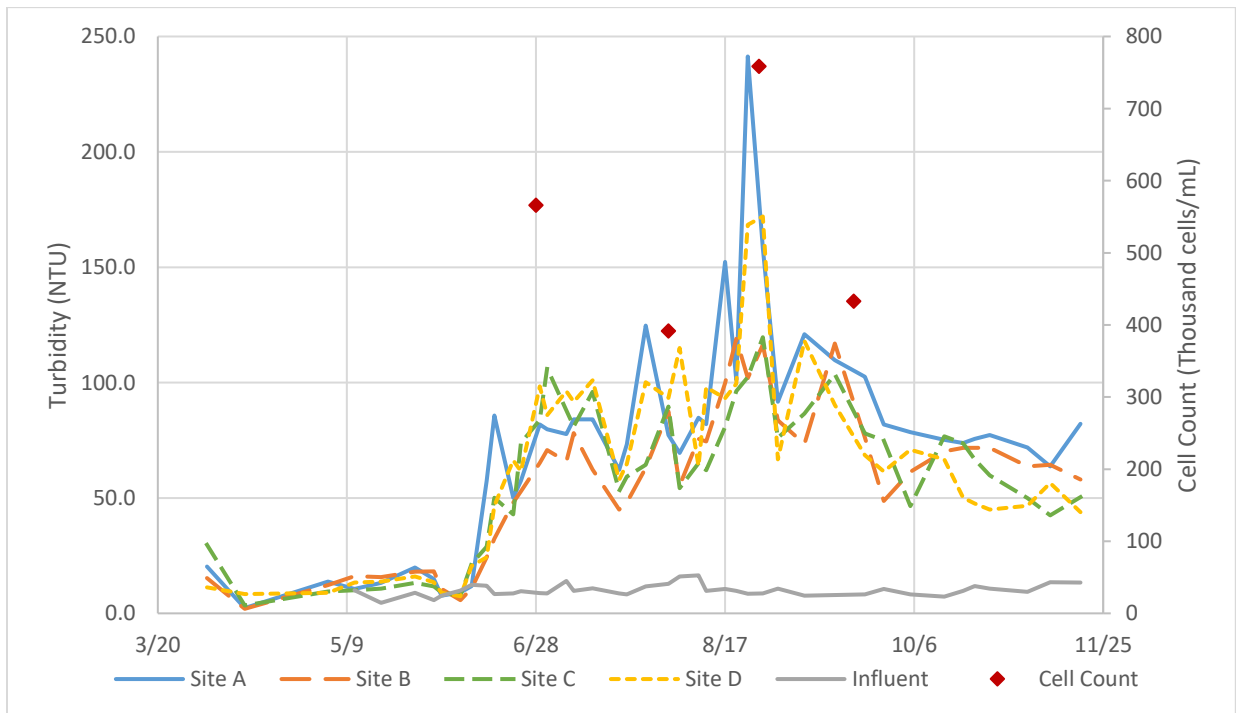


Figure 5.7: Turbidity and Cell Count Data

Turbidity measurements taken in the field were compared with cell count data provided by the Kansas Department of Health and Environment (KDHE) and a strong positive correlation was found ($r^2=0.87$) indicating turbidity can be used as a general indicator of the bloom severity in this study. KDHE sampling data is collected at Site's B and C.

Turbidity increased linearly during the first five weeks of the bloom event, then experienced nearly logarithmic growth in mid-August. At the end of sampling, turbidity measurements never reached pre-bloom levels. This can potentially be attributed to an increase in wind and adverse weather during this time influencing turbidity measurements through the addition of inorganic material. The pre-bloom turbidity may have been lower due to overwinter freezing of algae that caused them to settle into pond sediment (Hudon et al., 2014). Influent turbidity stayed relatively constant around 10 NTU and was not influenced by the bloom event.

Water Temperature

Water temperature readings were consistent between Sites A - D with no localized hot or cold spots throughout the Gathering Pond, see Figure 5.8.

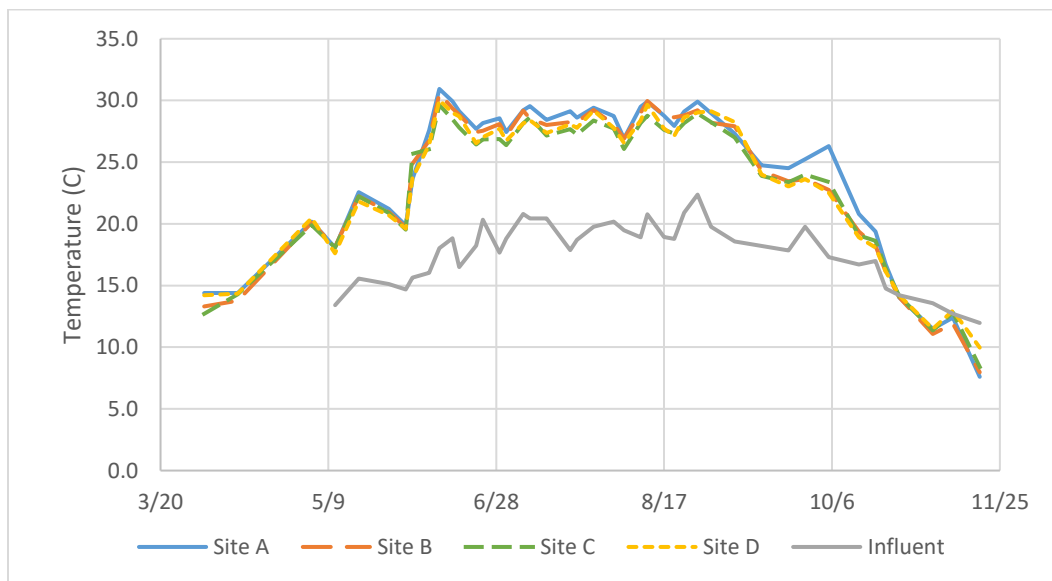


Figure 5.8: Water Temperature Data

The monitored HAB event coincided with the increase in water temperature to over 25 °C. Algae and algae-like bacteria generally proliferate at higher temperatures, with optimal temperatures ranging from 20 – 32 °C (H. W. Paerl, 1988; H. W. Paerl et al., 2011; H. W. Paerl & Huisman, 2008). Warm temperatures in surface water also increase vertical stratification and reduce mixing which create optimal growth conditions for algae (H. W. Paerl & Huisman, 2008). However, the bloom persisted well into the Fall, even with water temperatures decreasing below the optimal growing conditions. Influent water temperature was consistently 8 to 10 °C below the average temperature of the Gathering Pond in the spring and summer; this is due to the influent source water being groundwater seepage from the Milford Lake Dam. In October, the surface water temperature began to be colder than the influent.

pH

The Milford Gathering Pond has moderately alkaline water; attributed to the alluvial aquifer which has high concentrations of calcium and bicarbonate as a result of the underlying geologic structure (Helgesen, 1996). pH increased dramatically at the onset of the HAB event, see Figure 5.9.

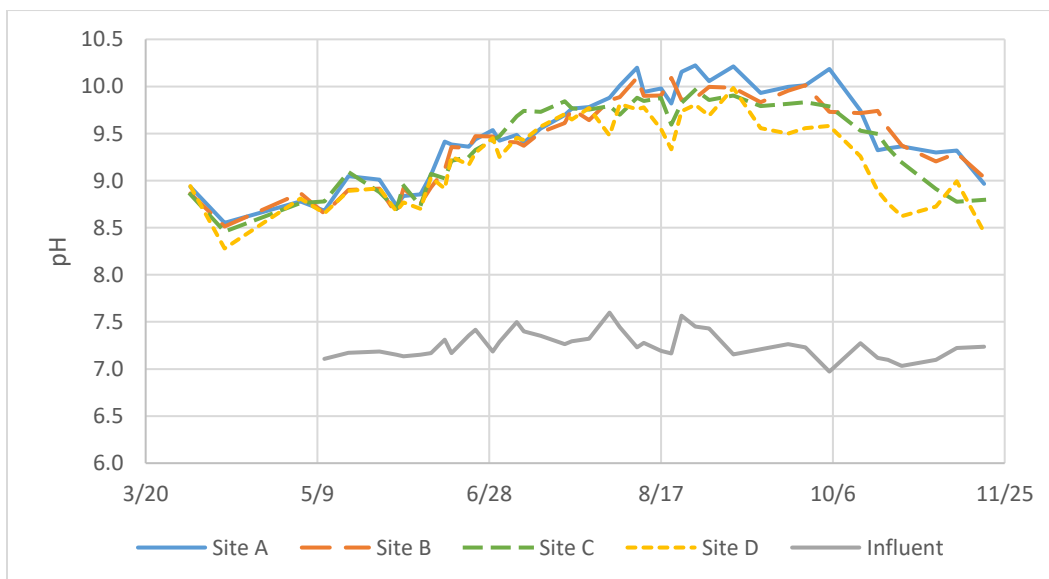


Figure 5.9: pH Data

From 4/12 to 8/10 pH increased by 1.54 ± 0.09 units. pH increase is most likely attributed to CO₂ depletion during photosynthesis, with pH values > 9 common during blooms (H. W. Paerl et al., 2011; Shumway et al., 2018; Rao et al., 2019). pH can even have a positive effect on growth rate of algae and further increase the severity of a bloom (Glibert et al., 2011; H. W. Paerl, 1988). The pH of the influent was not influenced by the bloom event and stayed relatively constant between 7 and 7.5. The pH of the influent does not match that of the surface water due to the source water coming through the engineered earthen dam with high silt and clay contents (Stark et al., 2011).

Orthophosphate

Overall, orthophosphate (Ortho-P) values were very high for the Milford Gathering Pond, with an average of 0.68 mg P/L. Natural levels of orthophosphate typically range from 0.005 – 0.05 mg P/L while orthophosphate levels of 0.08 mg P/L to 0.10 mg P/L have been shown to favor algal blooms (Ballah et al., 2019). Concentrations of orthophosphate are influenced by nutrient inputs, suspended particulate phosphorous in the water column, and resuspension of bottom sediments. The Gathering Pond has high nutrient loading from the seepage through the Milford Dam. Sediments at the base of the dam were found to have Ortho-P concentrations of up to 0.9196 mg P/L in 1986 and nutrients have only been accumulating behind the dam since then (Huggins & Howick, 1998). Ortho-P concentrations in the Gathering Pond are likely also influenced by windy conditions that cause mixing of the water column and upwelling of bottom sediment.

Ortho-P showed a steady increase before the bloom event, then rapidly decreased once the bloom event started, see Figure 5.10. As the algae reproduce, they consume the available phosphorous which causes levels to drop (Yao et al., 2020). Once the bloom started to decline,

Ortho-P began to raise to pre-bloom levels as the decaying algal biomass released their phosphorus back into the Gathering Pond or into bottom sediments (Lee et al., 2015). Sites C and D had consistently higher Ortho-P concentrations at the end of the sampling period that those measured at Sites A and B. This aligns with the turbidity data showing that Sites A and B had higher turbidity than Sites C and D during the overall decline of the bloom. It is likely, that the algae in Site A and B have not yet released their Ortho-P back into the Gathering Pond. Influent Ortho-P concentrations were variable and did not show any consistent trend with bloom progression dynamics over the duration of the sampling period.

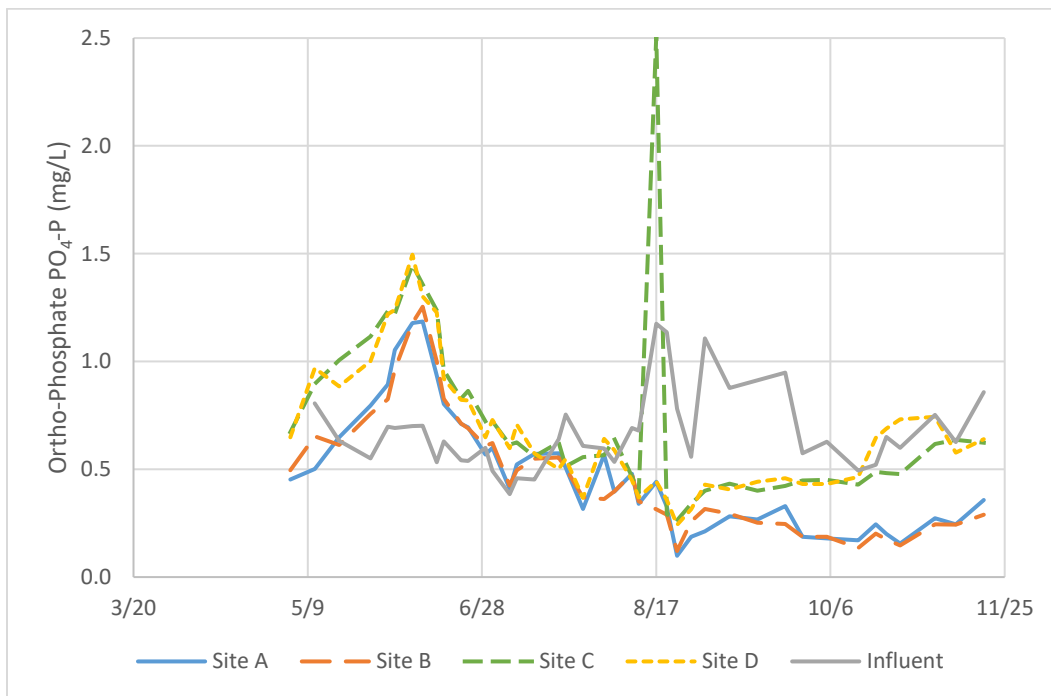


Figure 5.10: Orthophosphate as PO₄-P

Discrete sampling of the influent lateral canals was completed on October 22, 2021. Results showed that influent sampling in lateral canal four was likely under representative of the total phosphorous inputs into the Gathering Pond, as shown in Table 5.1. Lateral Canal 1 had no observed flow throughout the duration of this study. Sampling data supports Huggins and

Howick’s (1998) conclusion that a nutrient plume exists behind the dam, with the largest concentrations of nutrients found in the center of the dam.

Table 5.1: Lateral Canal Ortho-P Investigation

	Lateral Canal #	PO ₄ -P (mg/L)
	4	0.651
	3	1.088
	2	0.708
	1	NA

Filtered Total Carbon

Total carbon (TC) was measured on the 1.5µm filtrate samples and is not representative of all TC in the sample. Data before 6/22 is considered unreliable due to equipment issues and hence is excluded from this analysis. As the bloom progressed and increased in severity total filtered carbon measurements decreased, and once the bloom severity started to decrease, as evidenced by a decrease in turbidity, the filtered carbon measurements began to increase again, shown in Figure 5.11. Eutrophication has a significant impact on the sedimentary TOC sink as algae produce, consume, and alter organic carbon (Fiskal et al., 2019). However, during blooms cell numbers increases along with the concentration of organic carbon associated with organic matter released from cells (Merel et al., 2013; H. W. Paerl, 1988). It is likely an increase in organic carbon should have been observed. True trends in organic carbon were obscured due to filtration prior to sampling.

Sites C and D had consistently higher values of filtered TC than Sites A and B; this may be due to their location upstream of A and B, closer to the influent. The bloom was also less

severe (in reference to turbidity measurements) at Sites B and C. The influent is shown to be a significant source of total filtered carbon into the Gathering Pond.

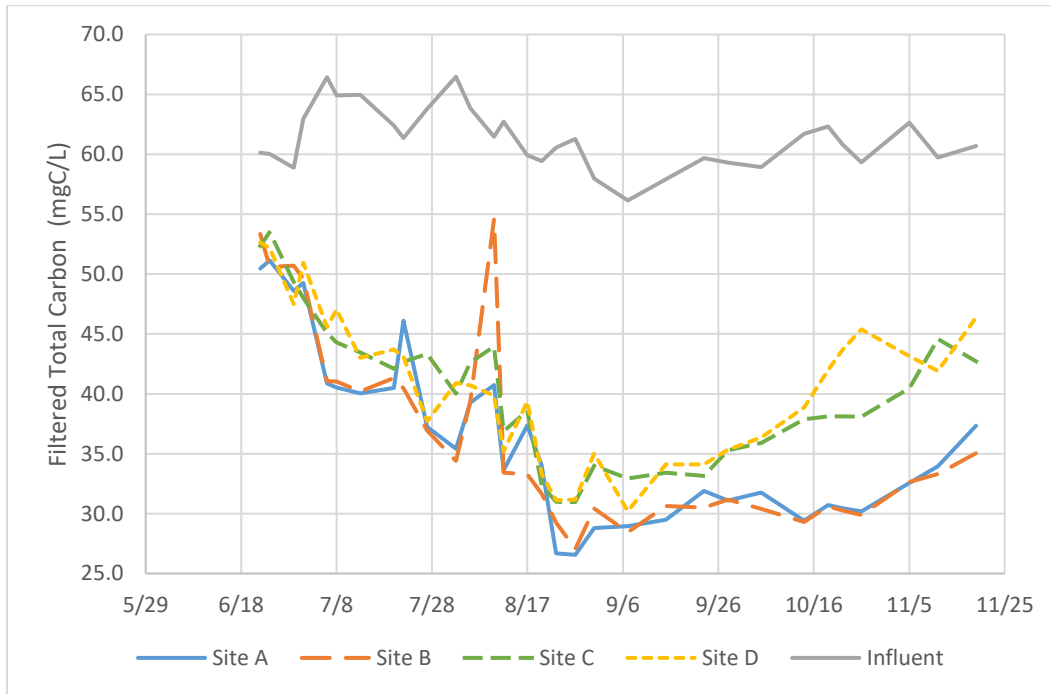


Figure 5.11: Filtered Total Carbon

Differences between filtered and unfiltered total carbon were investigated for samples collected on November 11th and 19th. Unfiltered total carbon in Sites A-D was on average 6.73 ± 2.68 mg C/L higher than filtered total carbon. Unfiltered total carbon in the influent was found to be greater than filtered total carbon by 0.21 ± 0.08 mg C/L. The results indicate that a large portion of carbon was excluded from the filtered samples, especially within the Gathering Pond.

Filtered Total Nitrogen

Total Nitrogen (TN) was also measured on the 1.5 μ m filtrate and is not representative of all TN in the sample. Data before 6/22 is considered unreliable due to equipment issues and is excluded from this analysis. Nitrogen and phosphorous are recognized as limiting nutrients leading to HAB proliferation. Algal and algae-like bacterial species have a wide diversity in their ability to use nitrogen and some have the capacity to fix nitrogen (Shumway et al., 2018).

We expected to see a decrease in nitrogen during the beginning of the bloom as algae consumed the available nitrogen (Lee et al., 2015). At the end of the bloom, the TN level should have increased as the algae died-off and released nitrogen back into the Gathering Pond. The recorded data shows total filtered nitrogen concentrations were variable and did not show any consistent trend, see Figure 5.12. The influent was a significant source of Nitrogen into the Gathering Pond which is consistent with the Ortho-P data likely suggesting seepage from the Milford Lake Dam having high nutrient concentrations due to the accumulation of nutrient rich sediment behind the dam (Huggins & Howick, 1998).

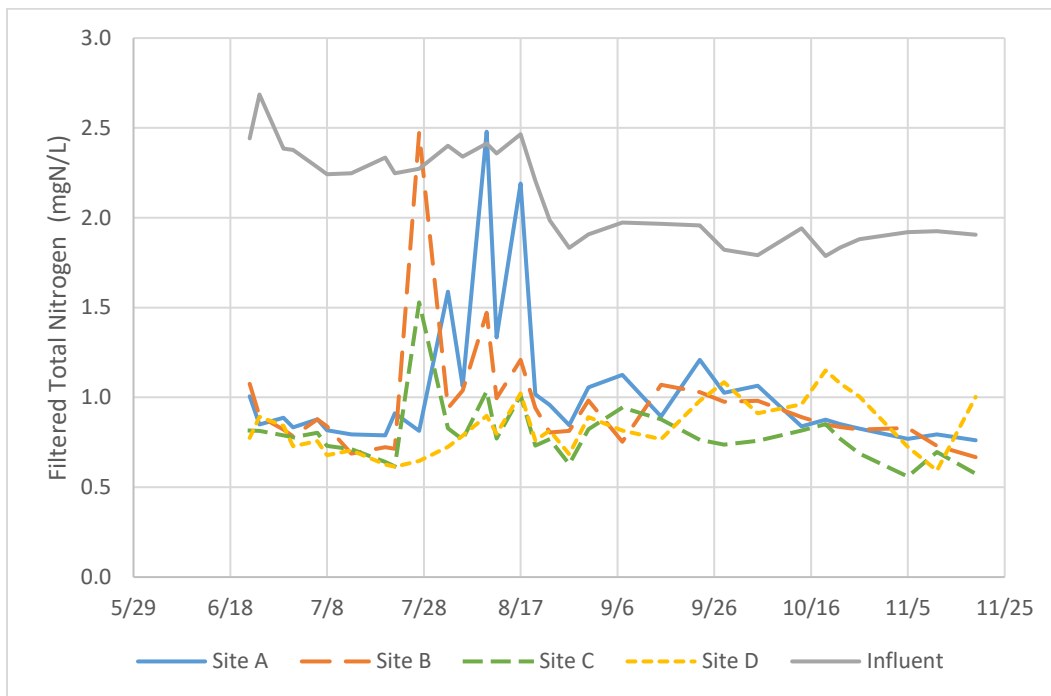


Figure 5.12: Filtered Total Nitrogen

Differences between filtered and unfiltered total nitrogen were investigated for samples collected on November 11th and 19th. Unfiltered total nitrogen in Sites A-D was on average 1.05 ± 0.44 mg N/L higher than filtered total nitrogen. The results indicate total nitrogen within the Gathering Pond was much higher than represented in the measured data.

Fluorescence Spectroscopy EEMs and PARAFAC Analysis

PARAFAC Components and Analysis

The fluorescent peaks identified in this study have many features in common with previously identified peaks found in algae impacted waters (Stedmon & Markager, 2005b; Villacorte et al., 2015; Khan et al., 2019; Wang et al., 2020; Yao et al., 2020). Characteristic fluorescence peaks identified in EEMs through PARAFAC include peaks A, C₁, C₂ T₁ and T₂, see Table 5.2.

Components 1 and 2 (Peaks A, C₁ and C₂) are similar to peaks associated with Humic acid-like materials common to a wide range of freshwater environments (Stedmon & Markager, 2005a). Peak A fluorescence has been observed in marine and terrestrial colored dissolved organic matter (CDOM) (Coble, 1996). Peak C is linked to humic material and can be linked to both terrestrially derived materials and those derived microbially (Khan et al., 2019).

Component 3 is similar to a T peak and is classified as Soluble Microbial by-product like compounds, specifically protein like compounds containing tryptophan (Coble, 1996; Chen et al., 2003). Tryptophan is an important organic carbon and nitrogen source for algae and microorganisms due to its high activity and is associated with biomass synthesis in surface water (Stedmon et al., 2003; Wang et al., 2020). Previous works have concluded that tryptophan peaks have high correlation to algal biomass and can therefore be used as an indicator of algal communities (Ziegmann et al., 2010; Xu et al., 2013).

PARAFAC identifies the maximum fluorescence, or F_{max} , within each component in the model. Due to the nature of the identified components having dual peaks, this F_{max} can be pulled from either peak. For example, for component 3, the maximum fluorescence can be from either the T1 or T2 peak. Components 1 and 2, representing humic-like compounds, showed no clear spatial or

temporal trends within Sites A – D. The influent was shown to be a significant source of humic compounds into the Gathering Pond. This corroborates the filtered total carbon data showing that the influent was a significant source of carbon, as humic materials are ~75% carbon.

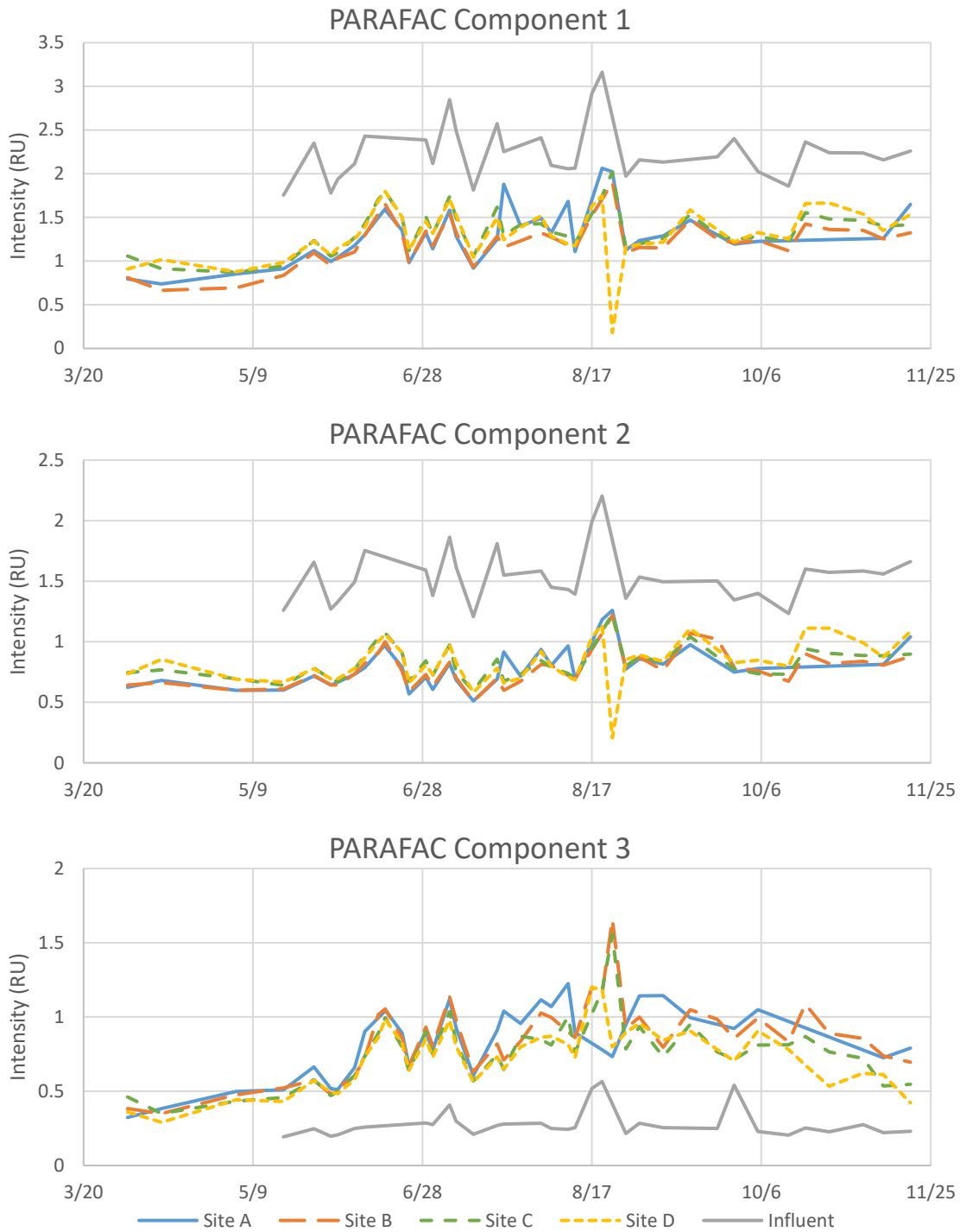
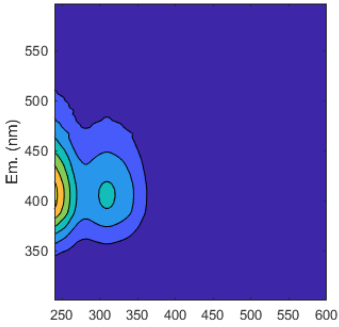
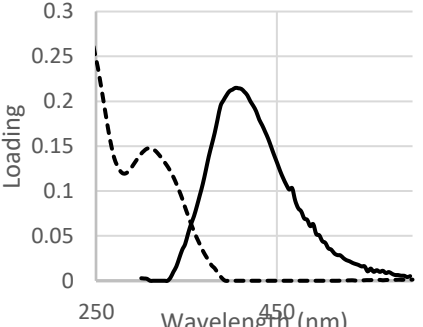
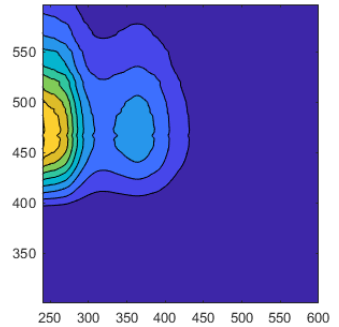
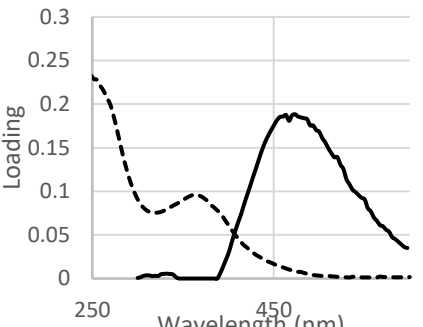
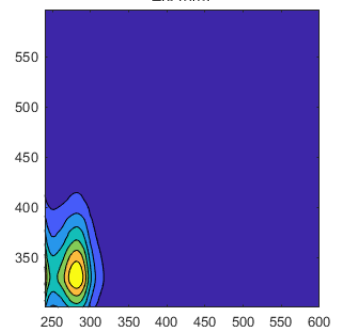
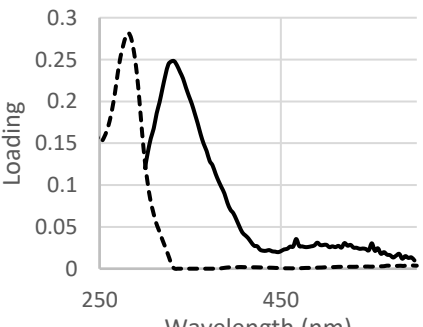


Figure 5.13: Fmax for Identified PARAFAC Components 1, 2, and 3

Component 3, representing tryptophan-like compounds, had high correlations with pH ($r^2=0.53$) and turbidity ($r^2=0.53$). This supports previous findings showing that the T peak is a good indicator of algal biomass, productivity, and the status of the algal biological community. During model calibration, the PARAFAC model identified that scans for Sites A and D during the peak were perceived fluorescence outliers. This is reflected in the Component 3 Site A and D F_{max} data at the peak of the bloom, with the fluorescence values significantly lower at the peak. In this case, PARAFAC does not do a good job representing tryptophan-like fluorescence at the peak of the bloom event and likely underestimates the maximum fluorescence.

PARAFAC modeling has many advantages and disadvantages. Some of the advantages to using PARAFAC modeling include that it is great for large datasets; its ability to identify obscured peaks and “bad” scans, and that it is mathematically validated. Because PARAFAC modeling involves splitting EEM fluorescence mathematically into a set of independent components, with the number of components determined by the EEM positioning, intensity, and type of organic matter within the data set, it is able to identify components that are not easily identifiable visually (Bro, 1997; Murphy et al., 2013). PARAFAC modeling also identifies “bad” scans or those with messy fluorescence data or high leverages and loadings which can then be removed from the dataset. Some of the disadvantages to using PARAFAC modeling include that it is time consuming, iterative, and intensive. Therefore, it is not reasonable to expect water managers to run a PARAFAC model on a small sample size over a short-time scale. Visual peak picking is a more viable option for tracking EEMs on a daily time scale and can be completed easily and rapidly by water managers.

Table 5.2: PARAFAC Identified Fluorescent Components within the Milford Gathering Pond

PARAFAC Component Label	Approximate EEM Location Ex(nm) : Em(nm)	Traditional Classification	EEM	Spectral Loading Ex(---) and Em (-)
Component 1 C1	Ex: <260 (300 – 325) Em: 390 - 410	Peak A + Peak C1		
Component 2 C2	Ex: <275 (350 – 360) Em: 475	Peak A + Peak C2		
Component 3 C3	Ex: <250 (280) Em: 325	Peak T1 + Peak T2		

Changes in EEM Spectra and Fluorescence Intensity for Visually Identified Peaks

Two peaks (C and T) were visually identified on the Gathering Pond EEMs. Only a C peak was identified in the influent and both a C peak and T peak were identified on the Gathering Pond EEMs and were consistently found in their respective samples throughout the duration of this study, see Figure 5.14.

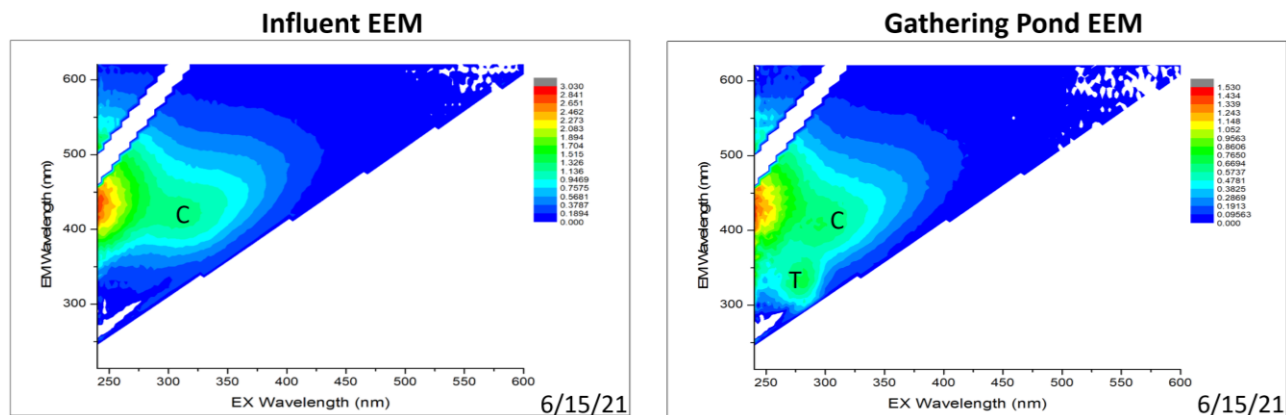


Figure 5.14: Comparison of Influent EEM and Gathering Pond EEM (Sites A-D)

The Raman Unit (RU) intensity for both peaks was tracked throughout the bloom. The visually determined T peak has high correlation with pH ($r^2=0.71$) and turbidity ($r^2=0.64$) and can be considered as a proxy indicator of bloom progress and severity. The T peak is not observed in the influent EEM further indicating that it is likely a result of biological activity of the algae as they proliferate. This T peak may also be attributed to sediment release, but wind conditions were consistent through the growth and peak of the bloom and did not increase until the last months of sampling. Influent intensity is not plotted with the T peak intensity because the T peak was not visually observed in influent EEMs. The C peak showed no clear trends throughout the duration of the bloom event. The C peak increases before the bloom starts, but stays relatively stable, oscillating between 0.6 and 0.8 Raman intensity units.

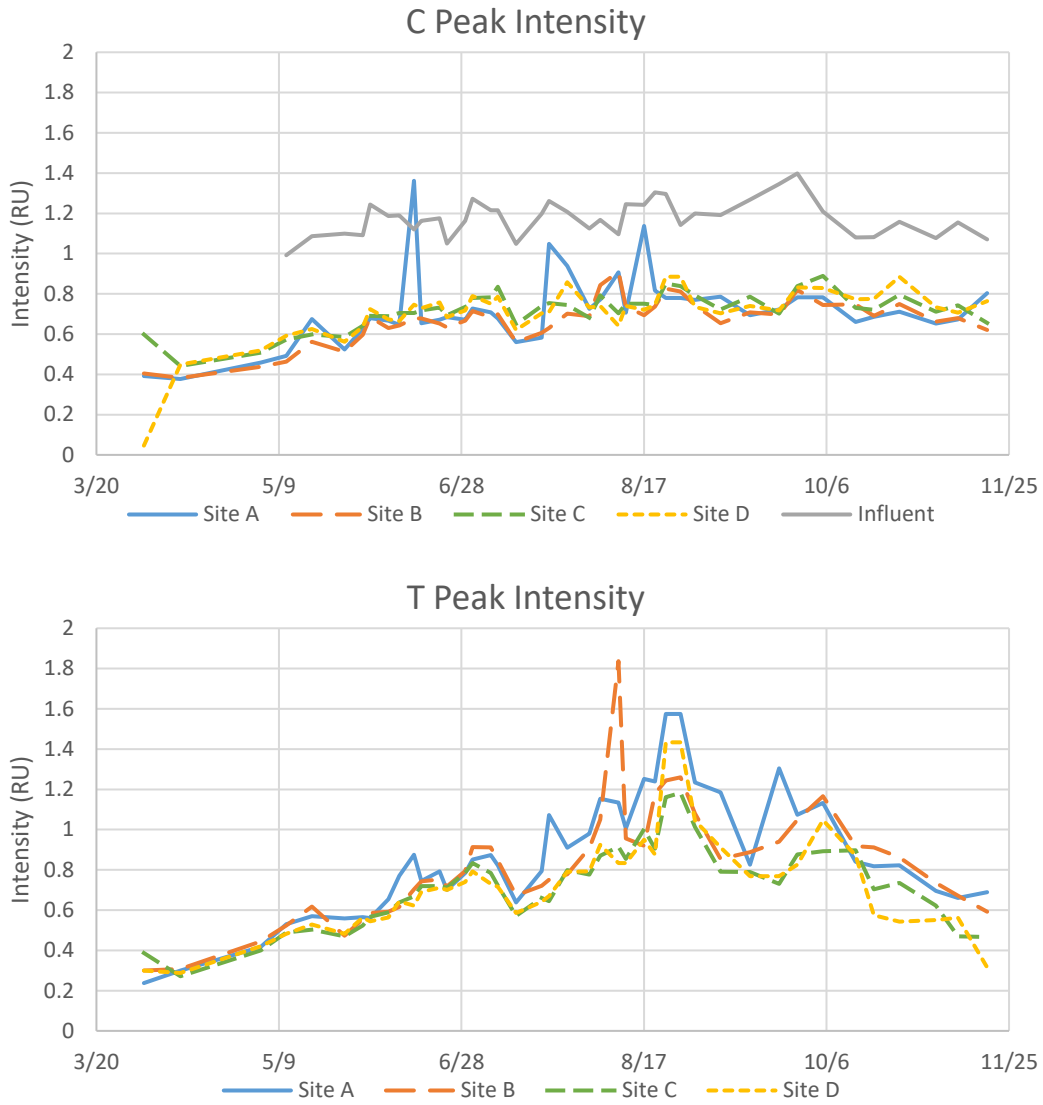


Figure 5.15: Visually Identified C and T Peak Intensities

T peak Intensity as a Predictive Indicator of Bloom Proliferation

T peaks have been associated with algal biological production in surface waters and are common in areas of high primary productivity (Hudson et al., 2007; Stedmon et al., 2003). The visually identified T peak intensity shows an increase in intensity before the bloom event starts with intensity increasing by 0.21 ± 0.08 RU during the month preceding the bloom, while PARAFAC Component 3 shows an increase of intensity of 0.47 ± 0.04 RU. This shows that EEMs pick up on changes in water chemistry before physical signs, i.e., a turbidity jump, of the

bloom are evident in the pond. In addition, the large rainfall event on July 15th did not affect the T peak intensity in the same way it effected turbidity.

In order for true prediction using the T peak, a baseline understanding of tryptophan-like fluorescence needs to be established. Seasonal influences and interferences should also be investigated and continuously monitored. Once established, any changes from the baseline intensity will be indicative of potential HAB events, or other water quality issues. An example baseline is shown in Figure 5.16.

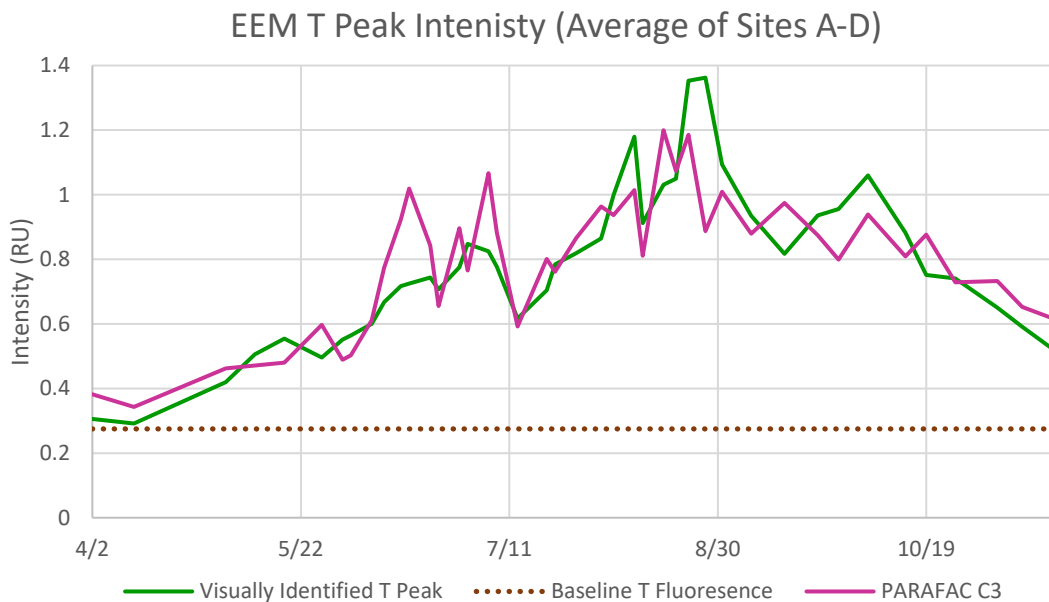


Figure 5.16: T Peak Intensity over Established Baseline

A comparison of the visually identified T peak intensity and the PARAFAC component 3 intensity show similar trends. However, PARAFAC does show higher variability than the visually identified fluorescence. Both the visually identified T peak intensity and the PARAFAC component 3 intensity have high correlations to pH and turbidity, although the visually identified T peak intensity has stronger correlations.

Visually identification of fluorescence peaks and manual tracking of peak intensity is the most useful approach for water managers because it permits tracing of small changes in water chemistry with a singular, rapid measurement. Fluorescence spectroscopy and the creation of EEMs is a straightforward process and requires no reactions or reagents. Results are available rapidly and visual peak identification can be completed quickly. Future in-situ monitoring of fluoresce and the establishment of a baseline fluorenones will allow a predictive indicator of blooms before they start, allowing for proactive rather than reactive mitigative strategies.

Correlations Between Parameters of Interest

Correlations (r^2) between turbidity, temperature, pH, orthophosphate, filtered TC, filtered TN, visually identified EEM peaks (Peak T and Peak C), and PARAFAC components (F_{max} for Components 1,2,3) were investigated, and visual representations of the correlation coefficients (r) were created using the Pearson correlation method. Blue represents a positive correlation while red represents a negative correlation. High correlations have more concentrated color and low correlations have less concentrated color. Correlations for the whole data set are detailed in Table 5.3 and summarized in Figure 5.17. The highest correlations ($r^2 > 0.6$) are the following: pH and turbidity ($r^2 = 0.64$), pH and Visually identified T Peak ($r^2 = 0.71$), Turbidity and Visually identified T Peak ($r^2 = 0.64$), Component 1 F_{max} and Component 2 F_{max} ($r^2 = 0.72$), and Visually identified T Peak and Component 3 F_{max} ($r^2 = 0.61$). The high correlations between visually identified T peak and turbidity and pH further supports the indication that the T peak is the best indicator of algal biological activity.

Table 5.3: Correlations (r^2) for Parameters of Interest

	pH	Temp	Turb.	Ortho-P	Filtered TC	Filtered TN	Peak T	Peak C	C1 Fmax	C2 Fmax	C3 Fmax
pH	-	0.29	0.64	0.44	0.20	0.04	0.71	0.35	0.05	0.03	0.53
Temp	-	-	0.08	0.02	0.01	0.11	0.21	0.07	0.01	0.01	0.23
Turb.	-	-	-	0.49	0.24	-	0.64	0.36	0.14	0.13	0.53
Ortho-P	-	-	-	-	0.17	0.05	0.30	0.12	0.02	0.04	0.14
Filtered TC	-	-	-	-	-	-	0.07	0.10	0.08	-	0.11
Filtered TN	-	-	-	-	-	-	0.06	0.09	-	-	0.08
T Peak	-	-	-	-	-	-	-	0.55	0.08	0.10	0.61
C Peak	-	-	-	-	-	-	-	-	0.28	0.18	0.48
C1 Fmax	-	-	-	-	-	-	-	-	-	0.72	0.52
C2 Fmax	-	-	-	-	-	-	-	-	-	-	0.42
C3 Fmax	-	-	-	-	-	-	-	-	-	-	-

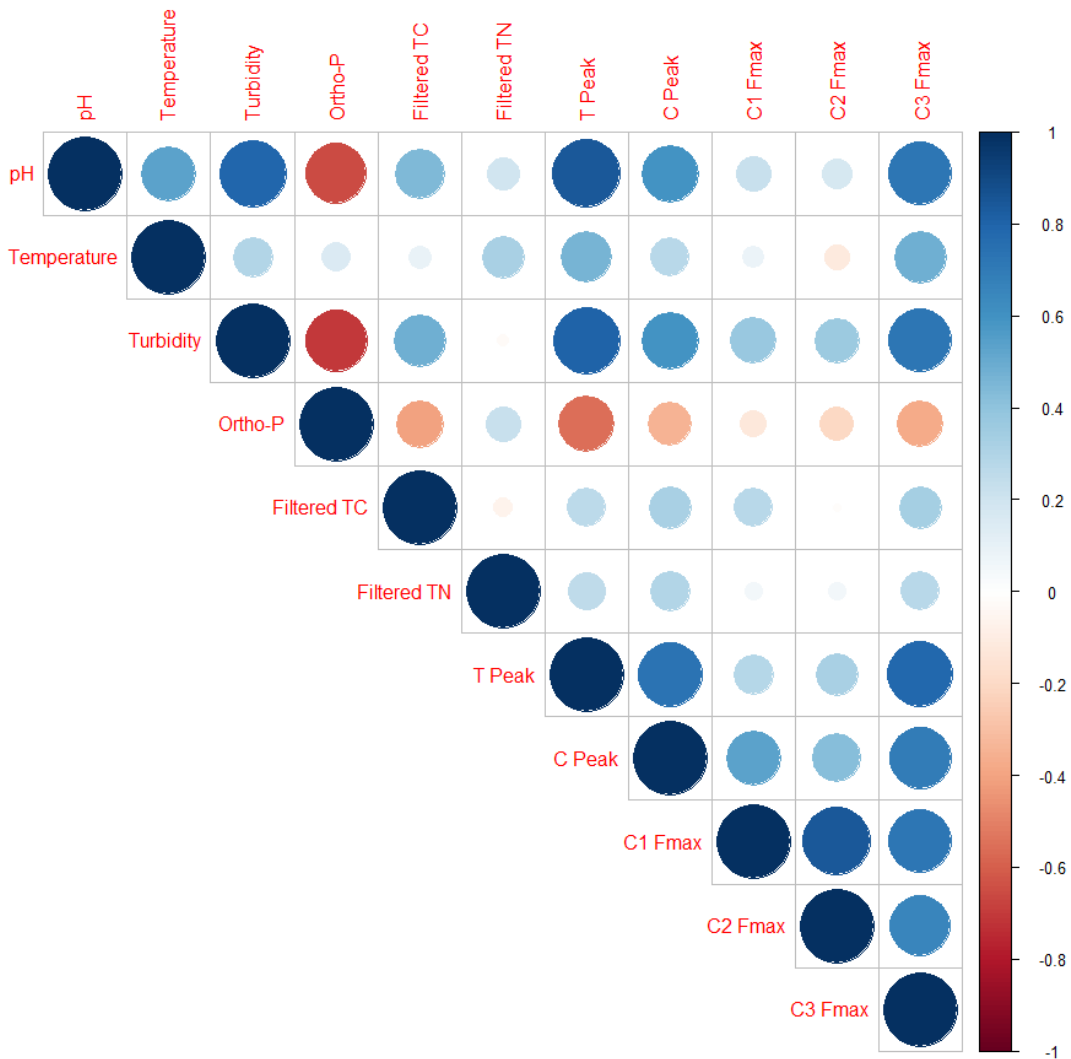


Figure 5.17: Correlation Coefficient (r) for all Parameters of Interest

Correlations for different phases of the bloom were also investigated. The bloom was broken down into three phases: pre-bloom phase (4/2 - 6/15), a bloom growth phase (6/17 – 8/23), and a bloom decline phase (8/27 – 11/19). Correlations for each phase are detailed in Table 5.4, with the highest correlations ($r^2 > 0.6$) highlighted in grey. A visual comparison between each phase is summarized in Figure 5.18. The pre-bloom phase showed many positive high correlations between all fluorescence parameters. Temperature, filtered TC, and turbidity all had high correlations with PARAFAC Components C1, C2, and C3. Temperature, orthophosphate, filtered TC and filtered TN had high correlations to the visually identified T peak. The bloom growth phase did not show many significant correlations between measured fluorescence and water quality parameters. This is likely because during bloom growth to bloom peak there was a lot of variation in algae proliferation and cycling, rainfall, and nutrient use. The visually identified T peak had high correlations to turbidity ($r^2=0.62$), but the same trend was not found with PARAFAC Component 3, which also represents the T peak. This is likely because the PARAFAC model identified many outliers during the bloom peak and caused maximum intensity to potentially be misrepresented during this time. In the bloom decline phase, the visually identified T peak had extremely high correlations with almost all water quality parameters. PARAFAC Components C1 and C2 had consistently high correlations throughout all bloom phases. This is likely attributed to their composition of humics changing similarly over time.

Table 5.4: Correlations (r^2) for Pre-Bloom, Growth, and Decline Phases

Pre-Bloom Phase (n=7)

	pH	Temp	Turb.	Ortho-P	Filtered TC	Filtered TN	Peak T	Peak C	C1 Fmax	C2 Fmax	C3 Fmax
pH	-	0.38	0.50	0.01	0.27	0.10	0.34	0.28	0.42	0.45	0.53
Temp	-	-	0.17	0.52	0.55	0.66	0.77	0.53	0.67	0.62	0.71
Turb.	-	-	-	0.00	0.24	0.01	0.36	0.44	0.58	0.66	0.64
Ortho-P	-	-	-	-	0.49	0.52	0.56	0.38	0.42	0.26	0.27
Filtered TC	-	-	-	-	-	0.42	0.64	0.27	0.62	0.58	0.64
Filtered TN	-	-	-	-	-	-	0.59	0.32	0.28	0.24	0.30
T Peak	-	-	-	-	-	-	-	0.83	0.76	0.64	0.71
C Peak	-	-	-	-	-	-	-	-	0.71	0.58	0.58
C1 Fmax	-	-	-	-	-	-	-	-	-	0.94	0.94
C2 Fmax	-	-	-	-	-	-	-	-	-	-	0.98
C3 Fmax	-	-	-	-	-	-	-	-	-	-	-

Bloom Growth Phase (n=18)

	pH	Temp	Turb.	Ortho-P	Filtered TC	Filtered TN	Peak T	Peak C	C1 Fmax	C2 Fmax	C3 Fmax
pH	-	0.19	0.29	0.42	0.14	0.18	0.53	0.35	-	0.01	0.11
Temp	-	-	0.12	0.17	0.30	0.04	0.11	0.08	0.01	0.01	0.07
Turb.	-	-	-	0.35	0.21	-	0.62	0.35	-	0.09	0.21
Ortho-P	-	-	-	-	0.10	-	0.36	0.15	-	-	0.01
Filtered TC	-	-	-	-	-	0.01	0.20	0.10	0.14	0.32	0.25
Filtered TN	-	-	-	-	-	-	0.08	0.19	0.01	0.01	0.14
T Peak	-	-	-	-	-	-	-	0.62	0.02	0.19	0.37
C Peak	-	-	-	-	-	-	-	-	0.07	0.14	0.36
C1 Fmax	-	-	-	-	-	-	-	-	-	0.79	0.62
C2 Fmax	-	-	-	-	-	-	-	-	-	-	0.77
C3 Fmax	-	-	-	-	-	-	-	-	-	-	-

Decline Phase (n=13)

	pH	Temp	Turb.	Ortho-P	Filtered TC	Filtered TN	Peak T	Peak C	C1 Fmax	C2 Fmax	C3 Fmax
pH	-	0.96	0.44	0.72	0.90	0.41	0.74	0.24	0.45	0.14	0.71
Temp	-	-	0.52	0.71	0.92	0.36	0.79	0.26	0.42	0.11	0.76
Turb.	-	-	-	0.36	0.66	-	0.52	0.12	0.16	-	0.29
Ortho-P	-	-	-	-	0.71	0.25	0.76	0.50	0.45	0.28	0.46
Filtered TC	-	-	-	-	-	0.25	0.77	0.22	0.35	0.09	0.66
Filtered TN	-	-	-	-	-	-	0.13	0.04	0.03	-	0.45
T Peak	-	-	-	-	-	-	-	0.50	0.55	0.23	0.52
C Peak	-	-	-	-	-	-	-	-	0.19	0.18	0.11
C1 Fmax	-	-	-	-	-	-	-	-	-	0.69	0.10
C2 Fmax	-	-	-	-	-	-	-	-	-	-	-
C3 Fmax	-	-	-	-	-	-	-	-	-	-	-

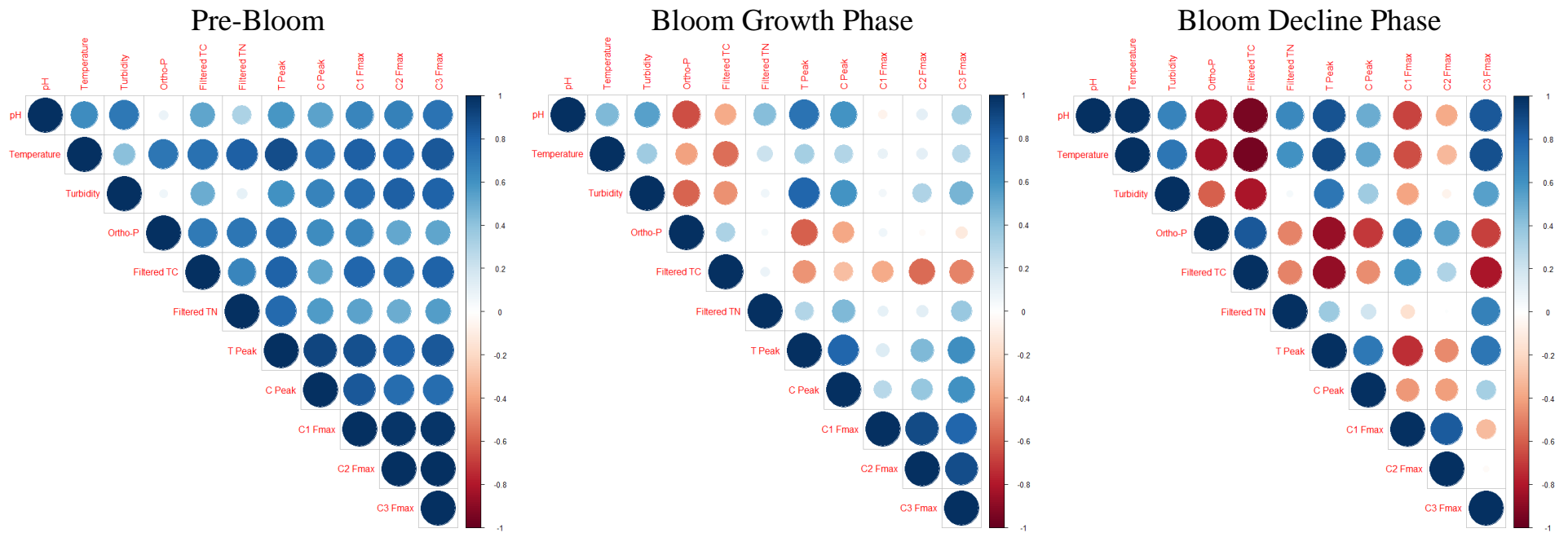


Figure 5.18: Correlation Coefficient (r) for Pre-Bloom, Bloom Growth, and Bloom Decline

Chapter 6 - Conclusion

The use of conventional algal bloom detection and monitoring is not robust enough to capture small changes in water quality and is often hampered by environmental interferences. The application of fluorescence spectroscopy for bloom detection and monitoring was found to be a more feasible option than traditional methods. Intensive monitoring and sampling of a complete HAB event in the Milford Gathering Pond proved both the feasibility of fluorescence spectroscopy as a tool for bloom monitoring and detection, but also as a predictive indicator of bloom development. Research outcomes have the potential to improve algal bloom monitoring and allow water managers to make more informed decisions to prevent or mitigate the effects of algal blooms. Earlier detection allows for intervention before blooms increase in severity, saving money on the cost of treatment, and keeping the ecosystem from degrading due to bloom proliferation, changing bloom mitigation and intervention to proactive rather than reactive process.

In depth analyses of fluorescence through visual peak identification and PARAFAC component analysis were both investigated. Although PARAFAC was able to identify more peaks, its intensive and iterative nature means that visual peak identification is better suited for water managers. The T peak representing tryptophan-like fluorescence was found to be the best indicator of algal activity and growth with significant correlations between the T peak and pH, turbidity, and orthophosphate. In addition, this supports previous works that concluded tryptophan-like fluorescence is the best indicator of algal biological activity. Increases in T peak intensity pre-dated bloom proliferation showing its ability to be a predictive indicator of bloom development, which would allow more proactive management of harmful algal blooms.

In the future, development of an online in-situ fluorescence spectroscopy device is needed, and the application and full-scale monitoring of large reservoirs needs to be investigated, as larger reservoirs have significantly lower levels of DOM than those found in the Milford Gathering Pond. In addition, a greater understanding of the fluorescence characteristics of algal species and their by-products is needed.

References

- Allen, M. R., Dube, O. P., Solecki, W., Aragón-Durand, F., Cramer, W., Humphreys, S., Kainuma, M., Kala, N., Mahowald, N., Mulugetta, Y., Perez, R., Wairiu, M., & Zickfeld, K. (2018). *Global Warming of 1.5°C. An IPCC Special Report on the impacts of global warming of 1.5°C above pre-industrial levels and related global greenhouse gas emission pathways, in the context of strengthening the global response to the threat of climate change, sustainable development, and efforts to eradicate poverty* (Framing and Context. In:). Intergovernmental Panel on Climate Change.
- Anderson, D. M. (2009). Approaches to monitoring, control, and management of harmful algal blooms (HABs). *Ocean & Coastal Management*, 52(7), 342–347. <https://doi.org/10.1016/j.ocecoaman.2009.04.006>
- Anderson, D. M., Glibert, P. M., & Burkholder, J. M. (2002). Harmful algal blooms and eutrophication: Nutrient sources, composition, and consequences. *Estuaries*, 25(4), 704–726. <https://doi.org/10.1007/BF02804901>
- Ballah, M., Bhoyroo, V., & Neetoo, H. (2019). Assessment of the physico-chemical quality and extent of algal proliferation in water from an impounding reservoir prone to eutrophication. *Journal of Ecology and Environment*, 43(1), 5. <https://doi.org/10.1186/s41610-018-0094-z>
- Bergman, L. E., Jones, K. L., & VanBriesen, J. M. (2020). Fluorescence characterization of organic matter and fouling: Case study in a full-scale reverse osmosis membrane treatment plant. *Water Environment Research*, 92(2), 161–172. <https://doi.org/10.1002/wer.1236>
- Beutler, M., Wiltshire, K. H., Meyer, B., Moldaenke, C., Lüring, C., Meyerhöfer, M., & Dau, H. (2002). A fluorometric method for the differentiation of algal populations in vivo and in situ. *Photosynthesis Research*, 72, 39–53.
- Brezonik, P. L., Bouchard, R. W., Finlay, J. C., Griffin, C. G., Olmanson, L. G., Anderson, J. P., Arnold, W. A., & Hozalski, R. (2019). Color, chlorophyll-a, and suspended solids effects on Secchi depth in lakes: Implications for trophic state assessment. *Ecological Applications*, 29(3). <https://doi.org/10.1002/eap.1871>
- Bro, R. (1997). PARAFAC. Tutorial and applications. *Chemometrics and Intelligent Laboratory Systems*, 38, 149–171.
- Brown, A. R., Lilley, M., Shutler, J., Lowe, C., Artioli, Y., Torres, R., Berdalet, E., & Tyler, C. R. (2019). Assessing risks and mitigating impacts of harmful algal blooms on mariculture and marine fisheries. *Reviews in Aquaculture*, 12, 1663–1688. <https://doi.org/10.1111/raq.12403>

- Brown, R. (1984). Relationships between suspended solids, turbidity, light attenuation, and algal productivity. *Lake and Reservoir Management*, 1(1), 198–205.
<https://doi.org/10.1080/07438148409354510>
- Chang, D.-W., Hobson, P., Burch, M., & Lin, T.-F. (2012). Measurement of cyanobacteria using in-vivo fluoroscopy – Effect of cyanobacterial species, pigments, and colonies. *Water Research*, 46(16), 5037–5048. <https://doi.org/10.1016/j.watres.2012.06.050>
- Chapra, S. C., Boehlert, B., Fant, C., Bierman, V. J., Henderson, J., Mills, D., Mas, D. M. L., Rennels, L., Jantarasami, L., Martinich, J., Strzeppek, K. M., & Paerl, H. W. (2017). Climate Change Impacts on Harmful Algal Blooms in U.S. Freshwaters: A Screening-Level Assessment. *Environmental Science & Technology*, 51(16), 8933–8943.
<https://doi.org/10.1021/acs.est.7b01498>
- Chen, W., Westerhoff, P., Leenheer, J. A., & Booksh, K. (2003). Fluorescence Excitation–Emission Matrix Regional Integration to Quantify Spectra for Dissolved Organic Matter. *Environmental Science & Technology*, 37(24), 5701–5710.
<https://doi.org/10.1021/es034354c>
- Coble, P. G. (1996). Characterization of marine and terrestrial DOM in seawater using excitation-emission matrix spectroscopy. *Marine Chemistry*, 51(4), 325–346.
[https://doi.org/10.1016/0304-4203\(95\)00062-3](https://doi.org/10.1016/0304-4203(95)00062-3)
- Coble, P. G. (2007). Marine Optical Biogeochemistry: The Chemistry of Ocean Color. *Chemical Reviews*, 107(2), 402–418. <https://doi.org/10.1021/cr050350+>
- Coble, P. G., Del Castillo, C. E., & Avril, B. (1998). Distribution and optical properties of CDOM in the Arabian Sea during the 1995 Southwest Monsoon. *Deep Sea Research Part II: Topical Studies in Oceanography*, 45(10–11), 2195–2223.
[https://doi.org/10.1016/S0967-0645\(98\)00068-X](https://doi.org/10.1016/S0967-0645(98)00068-X)
- Cory, R. M., Miller, M. P., McKnight, D. M., Guerard, J. J., & Miller, P. L. (2010). Effect of instrument-specific response on the analysis of fulvic acid fluorescence spectra. *Limnology and Oceanography: Methods*, 8, 67–78.
<https://doi.org/10.4319/lom.2010.8.0067>
- Dawson, J. (2011). Quick Response Is Key to Solving Taste-and-Odor Problems. *Opflow*, 37(10), 20–21. <https://doi.org/10.1002/j.1551-8701.2011.tb02372.x>
- Fellman, J. B., Hood, E., & Spencer, R. G. M. (2010). Fluorescence spectroscopy opens new windows into dissolved organic matter dynamics in freshwater ecosystems: A review. *Limnology and Oceanography*, 55(6), 2452–2462.
<https://doi.org/10.4319/lo.2010.55.6.2452>
- Ferrando, Noelia F., Benítez, Hernán H., Gabellone, Néstor A., Claps, María C., & Altamarino, Pablo R. (2015). A quick and effective estimation of algal density by turbidimetry developed with *Chlorella vulgaris* cultures. *Limnetica*, 34, 397–406.
<https://doi.org/10.23818/limn.34.30>

- Ferrão-Filho, A. da S., & Kozłowsky-Suzuki, B. (2011). Cyanotoxins: Bioaccumulation and Effects on Aquatic Animals. *Marine Drugs*, 9(12), 2729–2772. <https://doi.org/10.3390/md9122729>
- Fiskal, A., Deng, L., Michel, A., Eickenbusch, P., Han, X., Lagostina, L., Zhu, R., Sander, M., Schroth, M. H., Bernasconi, S. M., Dubois, N., & Lever, M. A. (2019). Effects of eutrophication on sedimentary organic carbon cycling in five temperate lakes. *Biogeosciences*, 16(19), 3725–3746. <https://doi.org/10.5194/bg-16-3725-2019>
- Gatz, L. (2019). *Freshwater Harmful Algal Blooms: Causes, Challenges, and Policy Considerations* (Congressional Research Service Report No. R44871; p. 30).
- Glibert, P. M., Fullerton, D., Burkholder, J. M., Cornwell, J. C., & Kana, T. M. (2011). Ecological Stoichiometry, Biogeochemical Cycling, Invasive Species, and Aquatic Food Webs: San Francisco Estuary and Comparative Systems. *Reviews in Fisheries Science*, 19(4), 358–417. <https://doi.org/10.1080/10641262.2011.611916>
- Graf, W. L. (1999). Dam Nation: A geographic census of American Dams and their large-scale hydrologic impacts. *Water Resources Research*, 35(4), 1305–1311.
- Graham, J. L., Dubrovsky, N. M., & Eberts, S. M. (2017). *Cyanobacterial Harmful Algal Blooms and U.S. Geological Survey Science Capabilities* (U.S. Geological Survey Open-File Report No. 1174; Open-File Report). U.S. Geological Survey. <https://pubs.er.usgs.gov/publication/ofr20161174>
- Hansen, A. M., Fleck, J. A., Kraus, T. E. C., Downing, B., von Dessenbeck, T., & Bergamaschi, B. A. (2018). *Procedures for Using the Horiba Scientific Aqualog® Fluorometer to Measure Absorbance and Fluorescence from Dissolved Organic Matter* (U.S. Geological Survey Open-File Report No. 2018–1096; Open-File Report, p. 31). U.S. Geological Survey. <https://doi.org/10.3133/ofr20181096>
- Helgesen, J. O. (1996). *Surface-water-quality assessment of the lower Kansas River basin, Kansas, and Nebraska; results of investigations, 1987-90* (U.S. Geological Survey Water-Supply Paper No. 2451). United States Geological Survey. <https://doi.org/10.3133/wsp2451>
- Henderson, R. K., Baker, A., Murphy, K. R., Hambly, A., Stuetz, R. M., & Khan, S. J. (2009). Fluorescence as a potential monitoring tool for recycled water systems: A review. *Water Research*, 43(4), 863–881. <https://doi.org/10.1016/j.watres.2008.11.027>
- Henderson, R. K., Baker, A., Parsons, S. A., & Jefferson, B. (2008). Characterisation of algogenic organic matter extracted from cyanobacteria, green algae, and diatoms. *Water Research*, 42(13), 3435–3445. <https://doi.org/10.1016/j.watres.2007.10.032>
- Henny, C., Jasalesmana, T., Kurniawan, R., Melati, I., Suryono, T., Susanti, E., Yoga, G. P., Rosidah, & Sudiono, B. (2020). The effectiveness of integrated floating treatment wetlands (FTWs) and lake fountain aeration systems (LFAS) in improving the landscape

- ecology and water quality of a eutrophic lake in Indonesia. *IOP Conference Series: Earth and Environmental Science*, 535, 1–15. <https://doi.org/10.1088/1755-1315/535/1/012018>
- Ho, J. C., & Michalak, A. M. (2020). Exploring temperature and precipitation impacts on harmful algal blooms across continental U.S. lakes. *Limnology and Oceanography*, 65(5), 992–1009. <https://doi.org/10.1002/lno.11365>
- Hudnell, H. K. (Ed.). (2008). *Cyanobacterial Harmful Algal Blooms: State of the Science and Research Needs* (Vol. 619). Springer New York. <https://doi.org/10.1007/978-0-387-75865-7>
- Hudnell, H. K. (2010). The state of U.S. freshwater harmful algal blooms assessments, policy, and legislation. *Toxicon*, 55(5), 1024–1034. <https://doi.org/10.1016/j.toxicon.2009.07.021>
- Hudon, C., De Sève, M., & Cattaneo, A. (2014). Increasing occurrence of the benthic filamentous cyanobacterium *Lyngbya wollei*: A symptom of freshwater ecosystem degradation. *Freshwater Science*, 33(2), 606–618. <https://doi.org/10.1086/675932>
- Hudson, N., Baker, A., & Reynolds, D. (2007). Fluorescence analysis of dissolved organic matter in natural, waste, and polluted waters—A review. *River Research and Applications*, 23(6), 631–649. <https://doi.org/10.1002/rra.1005>
- Huggins, D. G., & Howick, G. L. (1998). Effects of a Large Kansas Reservoir on Downstream Groundwater Quality. *Lake and Reservoir Management*, 14(1), 86–91. <https://doi.org/10.1080/07438149809354112>
- Kansas Mesonet*. (2021). Kansas Mesonet Historical Data. <http://mesonet.k-state.edu/weather/historical>
- Khan, S., Zamyadi, A., Rao, N. R. H., Li, X., Stuetz, R. M., & Henderson, R. K. (2019). Fluorescence spectroscopic characterisation of algal organic matter: Towards improved in situ fluorometer development. *Environmental Science: Water Research & Technology*, 5(2), 417–432. <https://doi.org/10.1039/C8EW00731D>
- Khan, W., Park, J. W., & Maeng, S. K. (2022). Fluorescence descriptors for algal organic matter and microalgae disintegration during ultrasonication. *Journal of Water Process Engineering*, 45, 102517. <https://doi.org/10.1016/j.jwpe.2021.102517>
- Klemas, V. (2012). Remote Sensing of Algal Blooms: An Overview with Case Studies. *Journal of Coastal Research*, 278, 34–43. <https://doi.org/10.2112/JCOASTRES-D-11-00051.1>
- Kong, Y., Zou, P., Song, L., Wang, Z., Qi, J., Zhu, L., & Xu, X. (2014). Effects of iron on the algae growth and microcystin synthesis: A review. *Ying Yong Sheng Tai Xue Bao*, 25(5), 1533–1540.
- Lawaetz, A. J., & Stedmon, C. A. (2009). Fluorescence Intensity Calibration Using the Raman Scatter Peak of Water. *Applied Spectroscopy*, 63(8), 936–940. <https://doi.org/10.1366/000370209788964548>

- Lee, T. A., Rollwagen-Bollens, G., & Bollens, S. M. (2015). The influence of water quality variables on cyanobacterial blooms and phytoplankton community composition in a shallow temperate lake. *Environmental Monitoring and Assessment*, 187(6), 315. <https://doi.org/10.1007/s10661-015-4550-2>
- Li, L., & Pan, G. (2013). A Universal Method for Flocculating Harmful Algal Blooms in Marine and Fresh Waters Using Modified Sand. *Environmental Science & Technology*, 47(9), 4555–4562. <https://doi.org/10.1021/es305234d>
- Lim, K., Evans, P. J., Utter, J., Malki, M., & Parameswaran, P. (2020). Dynamic monitoring and proactive fouling management in a pilot scale gas-sparged anaerobic membrane bioreactor. *Environmental Science: Water Research & Technology*, 6(10), 2914–2925. <https://doi.org/10.1039/D0EW00608D>
- Liu, D., Wang, P., Wei, G., Dong, W., & Hui, F. (2013). Removal of algal blooms from freshwater by the coagulation–magnetic separation method. *Environmental Science and Pollution Research*, 20(1), 60–65. <https://doi.org/10.1007/s11356-012-1052-4>
- Lopez, C. B., Jewett, E. B., Dortch, Q., Walton, B. T., & Hudnell, H. K. (2008). *Scientific Assessment of Freshwater Harmful Algal Blooms* (Interdisciplinary Working Group on Harmful Algal Blooms, Hypoxia, and Human Health of the Joint Subcommittee on Ocean Science and Technology).
- McQuaid, N., Zamyadi, A., Prévost, M., Bird, D. F., & Dorner, S. (2011). Use of in vivo phycoerythrin fluorescence to monitor potential microcystin-producing cyanobacterial biovolume in a drinking water source. *J. Environ. Monit.*, 13(2), 455–463. <https://doi.org/10.1039/C0EM00163E>
- Merel, S., Walker, D., Chicana, R., Snyder, S., Baurès, E., & Thomas, O. (2013). State of knowledge and concerns on cyanobacterial blooms and cyanotoxins. *Environment International*, 59, 303–327. <https://doi.org/10.1016/j.envint.2013.06.013>
- Molinari, B., Stewart-Koster, B., Adame, M. F., Campbell, M. D., McGregor, G., Schulz, C., Malthus, T. J., & Bunn, S. (2021). Relationships between algal primary productivity and environmental variables in tropical floodplain wetlands. *Inland Waters*, 11(2), 180–190. <https://doi.org/10.1080/20442041.2020.1843932>
- Murphy, K. R., Butler, K. D., Spencer, R. G. M., Stedmon, C. A., Boehme, J. R., & Aiken, G. R. (2010). Measurement of Dissolved Organic Matter Fluorescence in Aquatic Environments: An Interlaboratory Comparison. *Environmental Science & Technology*, 44(24), 9405–9412. <https://doi.org/10.1021/es102362t>
- Murphy, K. R., Stedmon, C. A., Graeber, D., & Bro, R. (2013). Fluorescence spectroscopy and multi-way techniques. PARAFAC. *Analytical Methods*, 5(23), 6557. <https://doi.org/10.1039/c3ay41160e>

- Murphy, K. R., Stedmon, C. A., Wenig, P., & Bro, R. (2014). OpenFluor– an online spectral library of auto-fluorescence by organic compounds in the environment. *Anal. Methods*, 6(3), 658–661. <https://doi.org/10.1039/C3AY41935E>
- Nebbioso, A., & Piccolo, A. (2013). Molecular characterization of dissolved organic matter (DOM): A critical review. *Analytical and Bioanalytical Chemistry*, 405(1), 109–124. <https://doi.org/10.1007/s00216-012-6363-2>
- Nutrient Pollution: Sources and Solutions* (EPA 820-F-15-096; A Compilation of Cost Data Associated with the Impacts and Control of Nutrient Pollution, p. IV–23). (2015). United States Environmental Protection Agency. <http://wrrfdata.org/NBP/Newsletter/wp-content/uploads/2015/06/EPA-Report-on-Cost-Data-Nutrient-Pollution-Control.pdf>
- Pacyna, J. M. (2008). Atmospheric Deposition. In *Encyclopedia of Ecology* (pp. 275–284). Elsevier Science.
- Paerl, H. (2014). Mitigating Harmful Cyanobacterial Blooms in a Human- and Climatically Impacted World. *Life*, 4(4), 988–1012. <https://doi.org/10.3390/life4040988>
- Paerl, H. (2018). Mitigating Toxic Planktonic Cyanobacterial Blooms in Aquatic Ecosystems Facing Increasing Anthropogenic and Climatic Pressures. *Toxins*, 10(2), 76. <https://doi.org/10.3390/toxins10020076>
- Paerl, H. W. (1988). Nuisance phytoplankton blooms in coastal, estuarine, and inland waters: Nuisance blooms. *Limnology and Oceanography*, 33(4part2), 823–843. <https://doi.org/10.4319/lo.1988.33.4part2.0823>
- Paerl, H. W., & Barnard, M. A. (2020). Mitigating the global expansion of harmful cyanobacterial blooms: Moving targets in a human- and climatically altered world. *Harmful Algae*, 96. <https://doi.org/10.1016/j.hal.2020.101845>
- Paerl, H. W., Hall, N. S., & Calandrino, E. S. (2011). Controlling harmful cyanobacterial blooms in a world experiencing anthropogenic and climatic-induced change. *Science of The Total Environment*, 409(10), 1739–1745. <https://doi.org/10.1016/j.scitotenv.2011.02.001>
- Paerl, H. W., & Huisman, J. (2008). Blooms Like It Hot. *Science*, 320(5872), 57–58. <https://doi.org/10.1126/science.1155398>
- Paerl, H. W., Scott, J. T., McCarthy, M. J., Newell, S. E., Gardner, W. S., Havens, K. E., Hoffman, D. K., Wilhelm, S. W., & Wurtsbaugh, W. A. (2016). It Takes Two to Tango: When and Where Dual Nutrient (N & P) Reductions Are Needed to Protect Lakes and Downstream Ecosystems. *Environmental Science & Technology*, 50(20), 10805–10813. <https://doi.org/10.1021/acs.est.6b02575>
- Piehl, M. (2008). Watershed management strategies to prevent and control cyanobacterial harmful algal blooms. *Advances in Experimental Medicine and Biology*, 619, 259–273.

- Ramadan, T. (2000). Algae Control Solves Aesthetic Problems. *Opflow*, 26(8), 1–4.
<https://doi.org/10.1002/j.1551-8701.2000.tb02264.x>
- Rao, S. M., Anthony, P., & Mogili Venkateswarlu, N. (2019). Biochemical Indicators of Algal Bloom in Sewage-Contaminated Lakes. *Journal of Hazardous, Toxic, and Radioactive Waste*, 23(4), 1–8. [https://doi.org/10.1061/\(ASCE\)HZ.2153-5515.0000459](https://doi.org/10.1061/(ASCE)HZ.2153-5515.0000459)
- Richardson, T. L., Lawrenz, E., Pinckney, J. L., Guajardo, R. C., Walker, E. A., Paerl, H. W., & MacIntyre, H. L. (2010). Spectral fluorometric characterization of phytoplankton community composition using the Algae Online Analyser®. *Water Research*, 44(8), 2461–2472. <https://doi.org/10.1016/j.watres.2010.01.012>
- Sands, K., & Wood, G. (2019). *Oversight of Animal Feeding Operations for Manure Management in the Great Lakes Basin* (170641 IJC Manure Management). International Joint Commission by the Great Lakes Water Quality Board.
- Sellner, K. G., Doucette, G. J., & Kirkpatrick, G. J. (2003). Harmful algal blooms: Causes, impacts, and detection. *Journal of Industrial Microbiology and Biotechnology*, 30(7), 383–406. <https://doi.org/10.1007/s10295-003-0074-9>
- Shumway, S. E., Burkholder, J. M., & Morton, S. L. (Eds.). (2018). *Harmful algal blooms: A compendium desk reference*. Wiley Blackwell.
- Shutova, Y., Baker, A., Bridgeman, J., & Henderson, R. K. (2014). Spectroscopic characterisation of dissolved organic matter changes in drinking water treatment: From PARAFAC analysis to online monitoring wavelengths. *Water Research*, 54, 159–169. <https://doi.org/10.1016/j.watres.2014.01.053>
- Singh, S. P., & Singh, P. (2015). Effect of temperature and light on the growth of algae species: A review. *Renewable and Sustainable Energy Reviews*, 50, 431–444. <https://doi.org/10.1016/j.rser.2015.05.024>
- Stark, T. D., Lewis, J. R., Castro, G., Walberg, F. C., & Mathews, D. L. (2011). Liquefaction subsurface investigation for Milford Dam. *Canadian Geotechnical Journal*, 48(10), 1504–1519. <https://doi.org/10.1139/t11-055>
- Stedmon, C. A., & Bro, R. (2008a). Characterizing dissolved organic matter fluorescence with parallel factor analysis: A tutorial: Fluorescence-PARAFAC analysis of DOM. *Limnology and Oceanography: Methods*, 6(11), 572–579. <https://doi.org/10.4319/lom.2008.6.572>
- Stedmon, C. A., & Bro, R. (2008b). Characterizing dissolved organic matter fluorescence with parallel factor analysis: A tutorial: Fluorescence-PARAFAC analysis of DOM. *Limnology and Oceanography: Methods*, 6(11), 572–579. <https://doi.org/10.4319/lom.2008.6.572>
- Stedmon, C. A., & Markager, S. (2005a). Resolving the variability in dissolved organic matter fluorescence in a temperate estuary and its catchment using PARAFAC analysis.

- Limnology and Oceanography*, 50(2), 686–697.
<https://doi.org/10.4319/lo.2005.50.2.0686>
- Stedmon, C. A., & Markager, S. (2005b). Tracing the production and degradation of autochthonous fractions of dissolved organic matter by fluorescence analysis. *Limnology and Oceanography*, 50(5), 1415–1426. <https://doi.org/10.4319/lo.2005.50.5.1415>
- Stedmon, C. A., Markager, S., & Bro, R. (2003). Tracing dissolved organic matter in aquatic environments using a new approach to fluorescence spectroscopy. *Marine Chemistry*, 82(3–4), 239–254. [https://doi.org/10.1016/S0304-4203\(03\)00072-0](https://doi.org/10.1016/S0304-4203(03)00072-0)
- Tang, Y. Z., Koch, F., & Gobler, C. J. (2010). Most harmful algal bloom species are vitamin B1 and B12 auxotrophs. *Proceedings of the National Academy of Sciences*, 107(48), 20756–20761. <https://doi.org/10.1073/pnas.1009566107>
- Thompson, J. K., Koseff, J. R., Monismith, S. G., & Lucas, L. V. (2008). Shallow water processes govern system-wide phytoplankton bloom dynamics: A field study. *Journal of Marine Systems*, 74(1–2), 153–166. <https://doi.org/10.1016/j.jmarsys.2007.12.006>
- Tomasko, D. A., Britt, M., & Carnevale, M. J. (2016). The ability of barley straw, cypress leaves and L-lysine to inhibit cyanobacteria in Lake Hancock, a hypereutrophic lake in Florida. *Florida Academy of Sciences, Inc*, 79(2/3), 147–158.
- U.S. EPA. (2004). *Risk Assessment Evaluation for Concentrated Animal Feeding Operations* (EPA/600/R-04/042). U.S. Environmental Protection Agency, Office of Research and Development, National Risk Management Research Laboratory.
- U.S. EPA. (2013). *Literature Review of Contaminants in Livestock and Poultry Manure and Implications for Water Quality* (Office of Water (4304T) EPA 820-R-13-002; p. 137). United States Environmental Protection Agency.
- Villacorte, L. O., Ekowati, Y., Neu, T. R., Kleijn, J. M., Winters, H., Amy, G., Schippers, J. C., & Kennedy, M. D. (2015). Characterisation of algal organic matter produced by bloom-forming marine and freshwater algae. *Water Research*, 73, 216–230.
<https://doi.org/10.1016/j.watres.2015.01.028>
- Vilsack, T., & Clark, C. Z. F. (2009). *2007 Census of Agriculture: United States Summary and State Data* (Volume 1 AC-07-A-51; Geographic Area Series). USDA.
nass.usda.gov/Publications/AgCensus/2007/Full_Report/Volume_1,_Chapter_1_US/usv1.pdf.
- Wang, S., Wang, W., Chen, J., Zhang, B., Zhao, L., & Jiang, X. (2020). Characteristics of Dissolved Organic Matter and Its Role in Lake Eutrophication at the Early Stage of Algal Blooms—A Case Study of Lake Taihu, China. *Water*, 12(8), 2278.
<https://doi.org/10.3390/w12082278>
- Williams, C. J., Yamashita, Y., Wilson, H. F., Jaffé, R., & Xenopoulos, M. A. (2010). Unraveling the role of land use and microbial activity in shaping dissolved organic matter

- characteristics in stream ecosystems. *Limnology and Oceanography*, 55(3), 1159–1171. <https://doi.org/10.4319/lo.2010.55.3.1159>
- Wurtsbaugh, W. A., Paerl, H. W., & Dodds, W. K. (2019). Nutrients, eutrophication, and harmful algal blooms along the freshwater to marine continuum. *Wiley Interdisciplinary Reviews: Water*, 6(5). <https://doi.org/10.1002/wat2.1373>
- Xu, H., Cai, H., Yu, G., & Jiang, H. (2013). Insights into extracellular polymeric substances of cyanobacterium *Microcystis aeruginosa* using fractionation procedure and parallel factor analysis. *Water Research*, 47(6), 2005–2014. <https://doi.org/10.1016/j.watres.2013.01.019>
- Yao, X., Zhang, Y., Zhang, L., Zhu, G., Qin, B., Zhou, Y., & Xue, J. (2020). Emerging role of dissolved organic nitrogen in supporting algal bloom persistence in Lake Taihu, China: Emphasis on internal transformations. *Science of The Total Environment*, 736, 139497. <https://doi.org/10.1016/j.scitotenv.2020.139497>
- Ye, L., Shi, X., Wu, X., Zhang, M., Yu, Y., Li, D., & Kong, F. (2011). Dynamics of dissolved organic carbon after a cyanobacterial bloom in hypereutrophic Lake Taihu (China). *Limnologica*, 41(4), 382–388. <https://doi.org/10.1016/j.limno.2011.06.001>
- Zamyadi, A., Choo, F., Newcombe, G., Stuetz, R., & Henderson, R. K. (2016). A review of monitoring technologies for real-time management of cyanobacteria: Recent advances and future direction. *TrAC Trends in Analytical Chemistry*, 85, 83–96. <https://doi.org/10.1016/j.trac.2016.06.023>
- Zepp, R. G., Sheldon, W. M., & Moran, M. A. (2004). Dissolved organic fluorophores in southeastern US coastal waters: Correction method for eliminating Rayleigh and Raman scattering peaks in excitation–emission matrices. *Marine Chemistry*, 89(1–4), 15–36. <https://doi.org/10.1016/j.marchem.2004.02.006>
- Zheng, Z., Zhang, W., Luo, X., Wang, S., Yang, X., He, J., & Nie, E. (2019). Design and Application of Plant Ecological Space Technology in Water Eutrophication Control. *Journal of Environmental Engineering*, 145(3), 04018142. [https://doi.org/10.1061/\(ASCE\)EE.1943-7870.0001485](https://doi.org/10.1061/(ASCE)EE.1943-7870.0001485)
- Zhou, S., Shao, Y., Gao, N., Deng, Y., Qiao, J., Ou, H., & Deng, J. (2013). Effects of different algaecides on the photosynthetic capacity, cell integrity and microcystin-LR release of *Microcystis aeruginosa*. *Science of The Total Environment*, 463–464, 111–119. <https://doi.org/10.1016/j.scitotenv.2013.05.064>
- Ziegmann, M., Abert, M., Müller, M., & Frimmel, F. H. (2010). Use of fluorescence fingerprints for the estimation of bloom formation and toxin production of *Microcystis aeruginosa*. *Water Research*, 44(1), 195–204. <https://doi.org/10.1016/j.watres.2009.09.035>
- Zielinski, O., Rüssmeier, N., Ferdinand, O., Miranda, M., & Wollschläger, J. (2018). Assessing Fluorescent Organic Matter in Natural Waters: Towards in Situ Excitation–Emission Matrix Spectroscopy. *Applied Sciences*, 8(12), 2685. <https://doi.org/10.3390/app8122685>

Appendix A - PARAFAC Identified Outliers

During PARAFAC analysis, leverages and loadings are used to identify “bad” emission scans. These scans may have messy excitation and emission graphs or those with high intensity outside of areas where peaks are expected. Once the outliers are plotted over the visually identified T peak, it is clear that some of the removed scans were likely valid, especially, Site B on August 20, 2021. However, some of the Site C and D scans at the beginning and end of the bloom show no clear indications that they are true outliers.

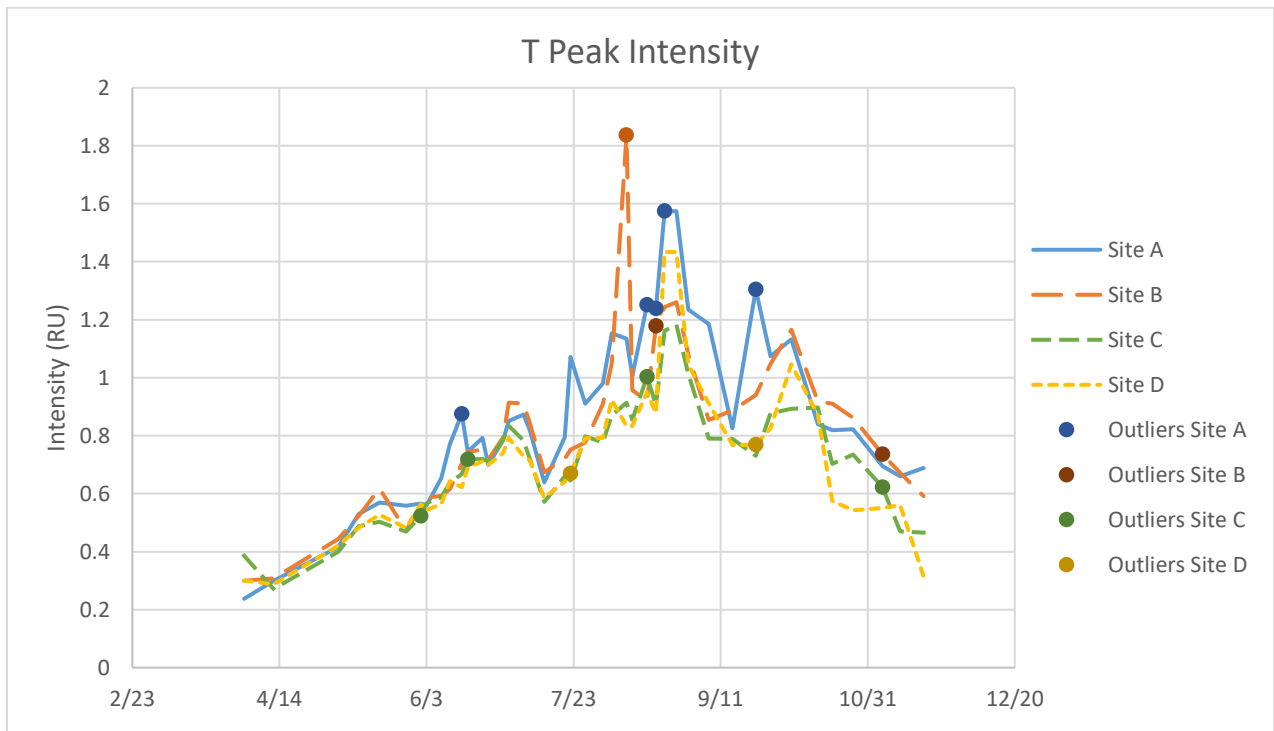


Figure A.1: PARAFAC Identified Outliers in Relation to Visually Identified T Peak

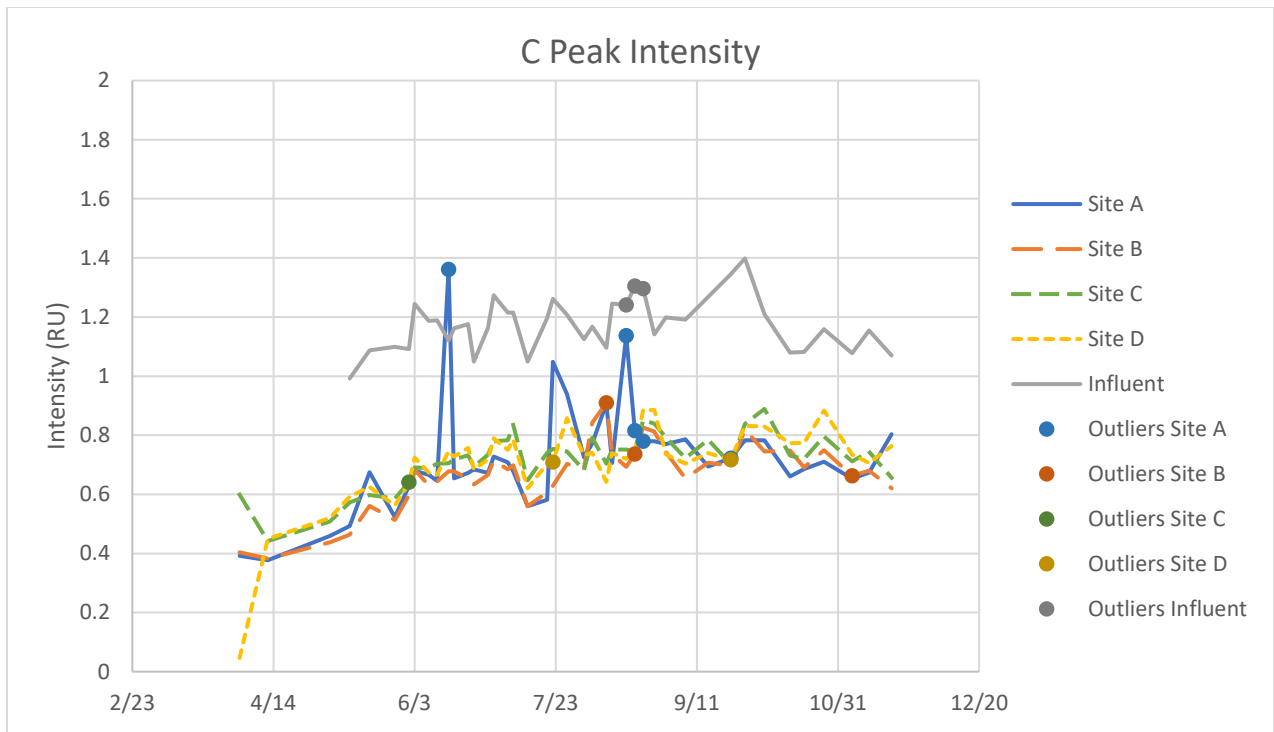


Figure A.2: PARAFAC Identified Outliers in Relation to Visually Identified T Peak

Table A.1: PARAFAC Identified Outliers

Site	Sample Date
Site A	June 15, 2021
	August 17, 2021
	August 20, 2021
	August 23, 2021
	September 23, 2021
Site B	August 10, 2021
	August 20, 2021
Site C	June 1, 2021
	June 17, 2021
	August 17, 2021
	October 5, 2021
Site D	July 22, 2021
	September 23, 2021
Influent	August 17, 2021
	August 20, 2021
	August 23, 2021